Article

Extending a Large-Scale Model to Better Represent Water Resources without Increasing the Model's Complexity

Robyn Horan [1,*], Nathan J. Rickards [1,*], Alexandra Kaelin [1], Helen E. Baron [1], Thomas Thomas [2], Virginie D. J. Keller [1], Prabhas K. Mishra [2], Manish K. Nema [2], Sekhar Muddu [3], Kaushal K. Garg [4], Rishi Pathak [2], Helen A. Houghton-Carr [1], Harry Dixon [1], Sharad K. Jain [5] and Gwyn Rees [1]

1 UK Centre for Ecology & Hydrology, Wallingford OX10 8BB, UK; akaelin.mail@gmail.com (A.K.); heron@ceh.ac.uk (H.E.B.); vke@ceh.ac.uk (V.D.J.K.); hahc@ceh.ac.uk (H.A.H.-C.); harr@ceh.ac.uk (H.D.); hgrees@ceh.ac.uk (G.R.)

2 National Institute of Hydrology, Roorkee 247667, India; thomas_nih@yahoo.com (T.T.); erprabhash@gmail.com (P.K.M.); mxnema@gmail.com (M.K.N.); rishicswe@gmail.com (R.P.)

3 Department of Civil Engineering, Indian Institute of Science, Bangalore 560012, India; sekhar.muddu@gmail.com

4 International Crops Research Institute for the Semi-Arid Tropics, Hyderabad 502324, India; K.GARG@cgiar.org

5 Civil Engineering Department, Indian Institute of Technology, Roorkee 247667, India; s_k_jain@yahoo.com

* Correspondence: robynhoran8@gmail.com (R.H.); natric@ceh.ac.uk (N.J.R.)

Abstract: The increasing impact of anthropogenic interference on river basins has facilitated the development of the representation of human influences in large-scale models. The representation of groundwater and large reservoirs have realised significant developments recently. Groundwater and reservoir representation in the Global Water Availability Assessment (GWAVA) model have been improved, critically, with a minimal increase in model complexity and data input requirements, in keeping with the model's applicability to regions with low-data availability. The increased functionality was assessed in two highly anthropogenically influenced basins. A revised groundwater routine was incorporated into GWAVA, which is fundamentally driven by three input parameters, and improved the simulation of streamflow and baseflow in the headwater catchments such that low-flow model skill increased 33–67% in the Cauvery and 66–100% in the Narmada. The existing reservoir routine was extended and improved the simulation of streamflow in catchments downstream of major reservoirs, using two calibratable parameters. The model performance was improved between 15% and 30% in the Cauvery and 7–30% in the Narmada, with the daily reservoir releases in the Cauvery improving significantly between 26% and 164%. The improvement of the groundwater and reservoir routines in GWAVA proved successful in improving the model performance, and the inclusions allowed for improved traceability of simulated water balance components. This study illustrates that improvement in the representation of human–water interactions in large-scale models is possible, without excessively increasing the model complexity and input data requirements.

Keywords: large-scale model; hydrology; groundwater; reservoirs; Cauvery; Narmada

1. Introduction

Humans are increasingly altering the hydrological cycle through the construction of reservoirs, changes in land-use, water abstractions, and urbanisation [1]. Accurate quantification of freshwater flows and storage is therefore important to support water management and governance in the near and far future [2]. Large-scale hydrological modelling estimates water fluxes, such as evapotranspiration, river discharge, and groundwater recharge, and water storage, including soil water, groundwater, and reservoirs [1,3,4] at a basin or continental scale.

Groundwater accounts for approximately one-third of total water withdrawals globally, and an estimated two billion people rely on groundwater as their primary source

of water. Additionally, more than half of the irrigation water globally is abstracted from groundwater sources [5]. It is therefore important to select a model that can accurately simulate the generation of groundwater, particularly in basins where the main source of baseflow depends upon groundwater storage [6].

A better representation of groundwater processes needs to be included in large-scale hydrological models to improve simulations and the understanding of feedback between the human and natural systems [7–9]. Simple one-dimensional groundwater routines currently exist within HiGW-MAT (Human Intervention and Groundwater coupled MAT-SIRO) [8], H08 [10], PCRaster GLOBal Water Balance (PCR-GLOBWB) [11], Community Water Model (CWatM) [12], WaterGAP [13], and Variable Infiltration Capacity (VIC) [14], with the focus on quantity and change in groundwater storage. Most models allow for groundwater to be recharged through rainfall, wetlands, and reservoirs. Groundwater abstractions are incorporated to meet demand. As far as the author is aware, none of these models, except VIC [9], consider lateral flow within the groundwater store without being fully coupled to MOD-FLOW [15]. Using MOD-FLOW significantly increases the data and computational requirements.

Approximately one-sixth of the annual river discharge globally available is stored because of the construction of an estimated 70,300 reservoirs [16]. Reservoir operations have a considerable impact on the natural discharge regime of a river. Simulating the available storage, volume, and timing of reservoir releases pose a significant challenge to hydrological modelling at a basin and continental scale [17]. Reservoir operational data are rarely freely available, if at all. Therefore, hydrological models include various schemes to estimate reservoir storage and releases.

A module that optimises reservoir outflow based on the operating purpose of the reservoir is included in VIC [18], WaterGAP [19], and H08 using the Hanasaki reservoir routine [20,21], and H08 has been updated to represent water transfers and local reservoirs [10]. The reservoir scheme used in Lund-Potsdam-Jena managed Land (LPJmL) [22] combines aspects used in H08 [21] and VIC [18]. Monthly target releases are calculated for each month of each operational year according to the primary purpose of the reservoir. The reservoir scheme in PCR-GLOBWB [11] is based on that included with VIC [18] but uses estimates of future inflows and demands via a weighted average of antecedent conditions. CWatM utilises a function of three storage limits and three outflow functions to determine reservoir releases. The storage limits are user-specified and depend on the physical characteristics of the reservoir. Other examples of recent reservoir routine implementations include, but are not limited to, the Soil & Water Assessment Tool (SWAT) [23], Distributed Hydrology Soil Vegetation Model (DHSVM) [17], VIC [9], Modélisation Environnementale Communautaire-Surface Hydrology (MESH) [24], and Hydrological Predictions for the Environment (HYPE) [25].

Although the above-mentioned models are useful tools, in this study, GWAVA is used because it is a water resource model specifically designed to work in low-data environments. GWAVA is a large-scale gridded water resource model [26] that accounts for natural hydrological processes (soils, land-use, and lakes), using a conceptual rainfall-runoff model and anthropogenic stresses (groundwater abstraction, irrigation, domestic and industrial demands, reservoir storage, and water transfers) via a demand-driven routine. The model can be run at a daily or monthly time scale and is adaptable to the data availability of the region. GWAVA was developed primarily for use in large, data-scarce regions. The model comprises only eleven mandatory parameters: four parameters pertaining to the physical parameters of the basin, three-time series pertaining to the climate variables (precipitation, potential evaporation, temperature), and four calibratable factors. The model further incorporates five reservoir parameters, nineteen water demand constraints, and six characteristics of mountains and glaciers that are optional input when the relevant data are available. GWAVA, however, does not comprehensively account for groundwater processes or regulated reservoir releases.

GWAVA has a simplistic representation of groundwater. The groundwater store for each grid cell receives groundwater recharge from the soil moisture storage and produces the baseflow component of streamflow. As a basic representation of deeper groundwater processes, water can drain from the groundwater store; this water is lost from the system. Water abstractions from the groundwater store are decoupled and are not abstracted in each time-step but summed at the completion of the run. GWAVA simulates regulated reservoir release using a non-linear equation utilising mean inflow, reservoir capacity, and two outflow parameters.

GWAVA has proven to be a useful tool for assessing water resource management; however, fundamental functionality for improving water resource estimations in highly anthropogenically influenced basins needs revision. With the increasing reliance on groundwater in semi-arid and arid regions and the continuous construction of major reservoirs globally, there is a critical need for water resource assessment tools to accurately consider these impacts, not only on the hydrological system but on water resource management. In line with existing large-scale models and the requirements to accurately represent highly anthropogenically influenced regions, this study aims to:

- Improve key components of GWAVA to better represent water management while maintaining low input data requirements and model complexity.
- Test the improvements in suitable basins to determine the success of the incorporated functionality.
- Use additional model output to gain insight into components of the basin water balance.

The GWAVA model is updated to better represent both groundwater abstraction, artificial recharge, and regulated reservoir releases. These updates are based largely on the principles of the AMBHAS-1D model and reservoir operations incorporating a routine derived from the Hanasaki reservoir routine.
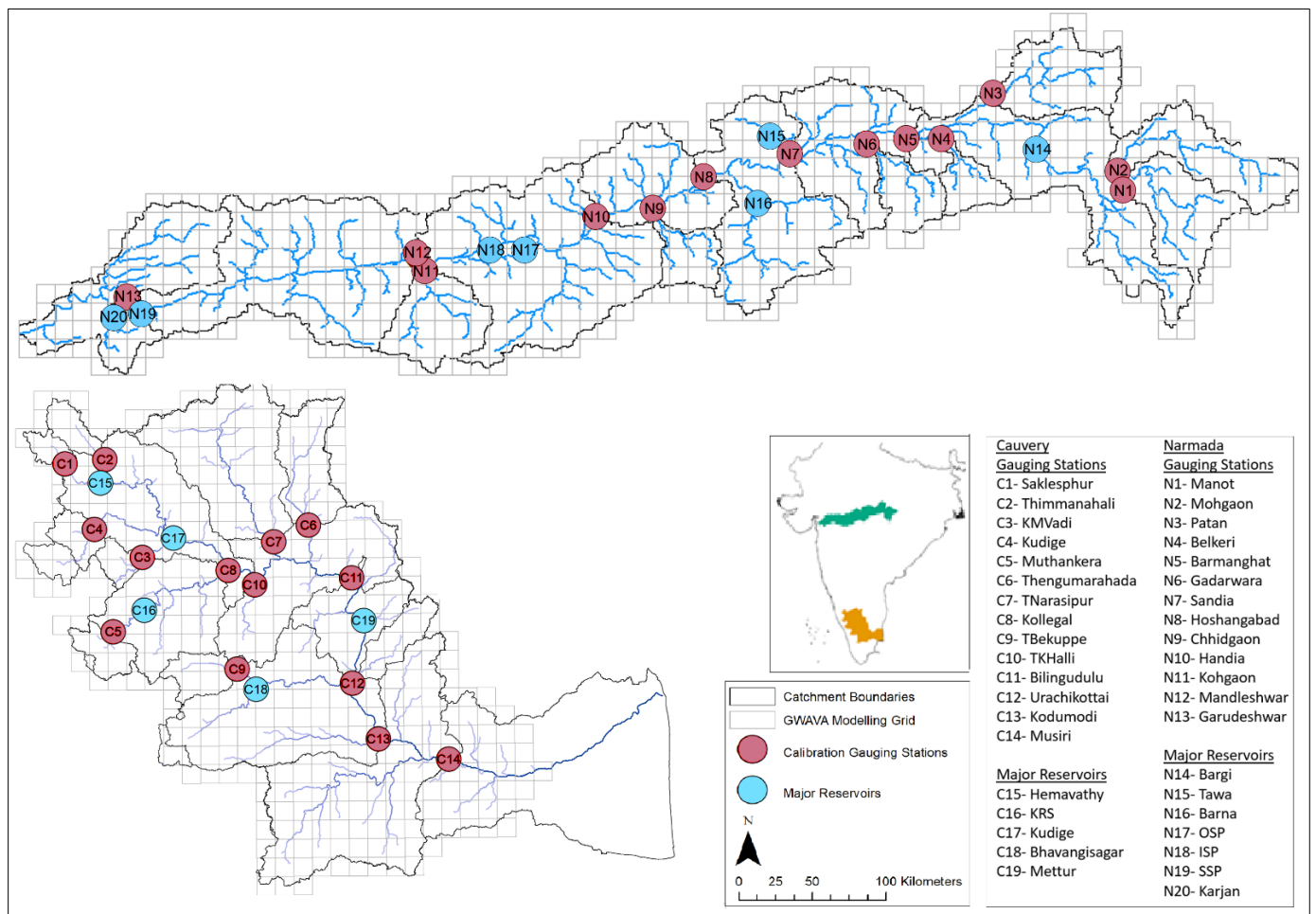
A groundwater routine based on AMBHAS-1D is included, introducing one calibratable parameter regarding the groundwater depth below ground level and two input parameters regarding the specific yield and depth of underlying geology. The Hanasaki equations are modified to allow for two calibratable outflow parameters to replace physical reservoir-engineering parameters. The addition of these two routines introduces only two input parameters and three calibratable parameters into the model.

The original model and the revised versions of the models are applied in two highly anthropogenically influenced basins, the Cauvery and Narmada Basins, India. The choice of the basin was based on the Cauvery being subjected to a high degree of groundwater pumping, while the Narmada houses three of the largest reservoirs in India. The overall model performance is evaluated using the Kling-Gupta Efficiency, while the model's ability to represent the low-flow periods is evaluated using the Log-Nash Efficiency at a sub-catchment scale. The change in reservoir outflows using the original GWAVA equation and the new modified Hanasaki equations is evaluated using the Nash-Sutcliffe Efficiency and the bias at the outlets of major reservoirs. Observed and simulated average sub-catchment groundwater and major reservoir storage levels are directly compared.

2. Methodology

2.1. Catchment Descriptions

The Cauvery and the Narmada basins (Figure 1) are situated in Peninsula India and are the fifth and sixth largest river basins in India, respectively. Both basins are snow-free, highly anthropogenically influenced, and reservoir-regulated to sustain the livelihoods of collective 45 million people. The basins experience a large degree of heterogeneity, not only in topography and land-use but also in climate and economic development [27].

Figure 1. Inset: the location of the Cauvery and Narmada Basins within India. Main maps: sub-catchment boundaries, modelling grid, and locations flow gauges used for calibration and major reservoirs within the Cauvery Basin and the Narmada Basin.

Both basins are highly regulated by reservoir releases, with a visible impact on downstream flows. The Narmada is sustained by the base flow through the dry periods, and the domestic and agricultural activities in the Cauvery are highly dependent on groundwater sources. Both basins suffer water scarcity, therefore the modelling and understanding of water resources are important for water management. Thus, it is critical that both reservoir releases and groundwater are accurately represented to undertake effective water resource modelling exercises.

The Cauvery is considered semi-arid, with the southwest (SW) monsoon supplying most of the water in the basin. The basin experiences distinct intra-annual seasons, namely, the SW monsoon between June and August, the northeast (NE) monsoon in September and October, and post-monsoon conditions in the winter. The upper basin receives rainfall from both the SW and NE monsoons, whereas the lower basin only receives rainfall from the NE monsoon. The mean annual rainfall varies from 6000 mm in the upper reaches to 300 mm on the eastern boundary. The mean daily temperatures vary between 9 and 25 °C throughout the basin [28]. The Western Ghats form a rain shadow along the western boundary, decreasing the precipitation gradient during the SW monsoon.

The current hydrological functioning of the Cauvery Basin has been significantly altered over the last century by water supply infrastructure, urbanisation, land-use change, and increased groundwater use. The Cauvery Basin is situated predominantly within the federal states of Karnataka and Tamil Nadu [28], and has been identified as highly water-stressed [29]. Despite rapidly developing urban and industrial centres, irrigation

throughout the basin requires approximately 90% of the total water resources [30]. The basin is highly regulated by aggressive groundwater pumping and reservoir release along the tributaries and main channel, with surface water flows only reaching the Bay of Bengal in years of strong monsoons [31]. Several hydrological modelling exercises have been conducted in the Cauvery Basin or sub-catchments thereof. Remote sensing methods [32], the artificial neutral network (ANN) model [32], GWAVA model [33,34], VIC model [34], and SWAT model [34,35] have been applied in various sub-catchments of the Cauvery. At a basin-scale, the SWAT [36–39], Soil Conservation Service Curve Number (SCS-CN) [40,41], and Variable Infiltration Capacity macroscale hydrological model (VIC- MHM) [42] have been used to simulate various components of the hydrological cycle.

The Narmada basin is subject to a tropical monsoon climate, with the southwest (SW) monsoon between July and September. The monsoon supplies over 75% of the basin's annual precipitation, with a rainfall gradient of 650 mm per annum to more than 1400 mm per annum in the upper regions. The mean daily temperatures vary between 18 and 32 °C throughout the basin.

The Narmada Basin is facing numerous resource management challenges, including state and sectoral competition for water. This highly regulated river flows through the states of Chhattisgarh, Madhya Pradesh, Maharashtra, and Gujarat, housing more than 250 dams of various sizes and purposes [43]. More than half of the basin is used for agriculture, with most of this land within designated irrigation command areas. The agriculture within the command areas is highly intensified, with an average cropping intensity of 135% [44]. The low flows in the basin are sustained by base flow and reservoir releases. The Narmada has been modelled at the basin-scale using the SCS-CN method [45], VIC-MHM [42], and geoinformatics [46]. Sub-catchments of the Narmada have been represented using SHE [47], SCS-CN [48–50], and SWAT [51]. The above-mentioned studies focussing on the Cauvery and the Narmada Basins highlight the minimal representation of anthropogenic influences, groundwater abstraction, and reservoir operations within the existing modelling exercises. GWAVA has been applied in both the Cauvery basin [33,34] and the Upper Narmada basin [52]. These publications highlight the need for a more comprehensive reservoir routine when modelling highly regulated basins, and for the inclusion of a coupled groundwater module to account for the limitations of natural groundwater resources and groundwater abstraction to meet anthropogenic demand.

2.2. Model Improvement

GWAVA has proven to be a useful tool for assessing water resource management, however, the model should be extended to include the representation of processes and to better represent groundwater and major reservoirs, due to the increasing reliance on groundwater in semi-arid and arid regions and the continuous construction of major reservoirs globally.

2.2.1. Representing Groundwater Processes

AMBHAS-1D [53] is a spatial groundwater model that determines a daily groundwater-level based on equations from McDonald & Harbaugh (1988) [54]. AMBHAS-1D implements distributed transient groundwater modelling. The model is based on the groundwater flow equation numerically solved, using the finite-difference scheme [55]. The implementation of various AMBHAS versions in India was found to be highly successful in simulating groundwater-levels across areas of Karnataka [56], in the Barembadi catchment [57,58] and an idealised system based on the River River [10]. Additionally, de Bruin et al. (2012) [59] utilised the results generated from AMBHAS-1D to guide the set of SWAT groundwater parameters for use in the Jaldhaka Basin. The successful application of AMBHAS-1D highlighted its suitability in India and other regions with low-data availability.

In line with the AMBHAS-1D conceptualisation, additional groundwater processes have been incorporated into GWAVA through the full coupling of the recharge, streamflow,

water abstractions, and base flow (Figure 2). The groundwater store was conceptualised as a vertically layered aquifer. Each layer was allocated a specific yield and depth and can vary from cell to cell based on data available about local hydrogeology. The aquifer can be recharged from soil moisture, the bottom of lakes, reservoirs, and small-scale recharge interventions and leaking via the water supply infrastructure. Water can be directly abstracted from the aquifer to its maximum depth. The groundwater contribution to baseflow (*BF*) was calculated as follows:

$$BF = \begin{cases} \gamma \times (GW_{store} - GW_{BF}), & GW_{store} > GW_{BF} \\ 0, & GW_{store} \leq GW_{BF} \end{cases} \quad (1)$$

where γ is the routing coefficient, GW_{store} is the groundwater store, and GW_{BF} is the level of groundwater storage below which there is no baseflow. GW_{BF} can be converted to an aquifer depth below ground level by dividing by the specific yield.
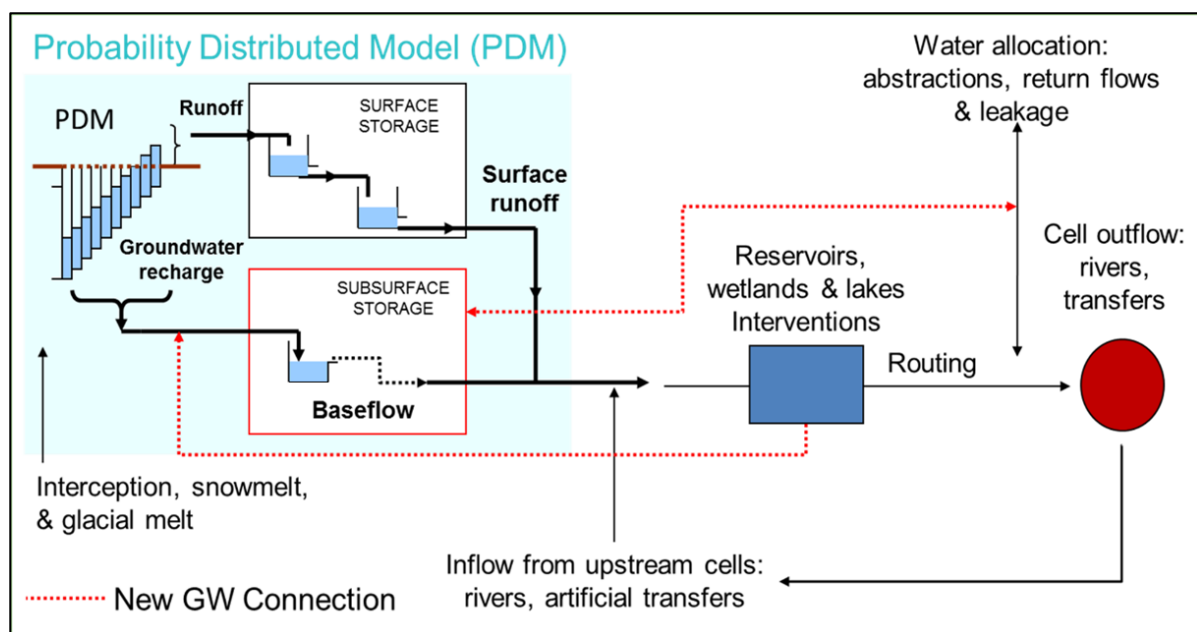

Figure 2. Schematic of the new groundwater (GW) connections and feedback included in the GWAVA model [60].

The implementation of the fully coupled groundwater functionality with GWAVA is flexible. The necessary input is limited to the specific yield and aquifer depth. In areas where data are limited, the aquifer characteristics can be agglomerated into a single layer, whereas, in regions with more comprehensive data the aquifer can be divided into more layers (with no upper limit).

2.2.2. Regulated Reservoirs

In practice, reservoir-operating rules are normally based on the specifications of each reservoir, the hydrometeorological conditions of the basin, and the water demand downstream. Hanasaki et al. (2006) [20] developed an algorithm to approximate reservoir-operating rules within global hydrological and land-surface models. The algorithm reflects these parameters and can be implemented with currently available global datasets (reservoir dimensions and purpose, simulated inflow, river discharge, water use, etc.).

A reservoir operation scheme is a valuable tool in regions where specific data about the reservoir characteristics of the outflow volumes are not available. The algorithm consists of two equations. The first is used when a consistent reservoir release is expected (i.e., when used for hydropower or to meet domestic demand), and the second is for a seasonal release (i.e., when used for irrigation).

For consistent release reservoirs, the operating rules are set to minimise inter-annual and seasonal reservoir releases. Hanasaki et al. (2006) [20] presents the equations as follows.

When the reservoir capacity divided by the mean annual inflow (*c*) is greater than 0.5:

$$r = \frac{S_{ini}}{0.85C} \times i_{mean} \tag{2}$$

When the reservoir capacity divided by the mean annual inflow (*c*) is less than or equal to 0.5:

$$r = \left(\frac{C}{0.5}\right)^2 \times \frac{S_{ini}}{0.85C} \times i_{mean} + \left[1 - \left(\frac{C}{0.5}\right)^2\right] \times i \tag{3}$$

where r is the simulated reservoir release (m^3/s), S_{ini} is the simulated storage at the beginning of the operational year (m^3), C is the user input reservoir capacity (m^3), i_{mean} is the simulated mean annual inflow (m^3/s) and, i is the simulated daily inflow (m^3/s).

This algorithm has been successfully incorporated into H08 [61] and influenced the reservoir routines of WATERGAP [1] and LPJmL [23]. The scheme is simple and designed primarily to represent inter-annual and monthly fluctuations in reservoir release. This approach has been demonstrated to be largely valid, but because reservoir operations are highly complex and tend to be based on human decisions, there is inevitably a level of uncertainty associated with its application.

The two new reservoir equations added to the GWAVA model are a simplified version of the Hanasaki equations [20], while the existing reservoir routine is maintained as an option [5]. Since GWAVA can account for irrigation water demand within the transfers' routine, the equations for consistent reservoir release have been implemented. In the original Hanasaki equation, i_{mean} was calculated as the mean inflow overall simulated years, as S_{ini} accounted for inter-annual variability. In Equation (5), i_{mean} has been changed to reflect the yearly mean inflow to introduce inter-annual variability.

When the reservoir capacity divided by the mean annual inflow (*c*) is greater than 0.5:

$$r = \alpha \times i_{am} \tag{4}$$

When the reservoir capacity divided by the mean annual inflow (*c*) is less than or equal to 0.5:

$$r = \alpha \times \beta \times i_{am} + [1 - \beta] \times i \tag{5}$$

where i_{am} is the mean yearly inflow (m^3/s) and α and β are user-set parameters between 0 and 1, replacing $\frac{S_{ini}}{0.85C}$ and $\left(\frac{C}{0.5}\right)^2$ from the original Hanasaki equations, respectively.

The user-set parameters can be manually calibrated to best fit either the observed streamflow at the next downstream gauging point of the reservoir or the reported reservoir outflow-data. The addition of the regulated reservoir routine includes an additional two calibratable parameters (α and β) and thus does not increase the input data required to incorporate this routine.

2.3. Data Acquisition

Input data were collected from several sources and extracted from global and regional datasets. The sources and details of the data used in this modelling exercise can be found in Tables A1 and A2, and in Appendix A.

2.4. Model Setup

The Cauvery and Narmada Basins were modelled at a spatial scale of 0.125 degrees using four different versions of the GWAVA model.

- GWAVA—the original version of GWAVA [5]
- GWAVA-GW—the original version of GWAVA with groundwater coupling

- GWAVA-Res—the original version of GWAVA with the regulated reservoirs
- GWAVA 5.1—the original version of GWAVA with both the groundwater coupling and regulated reservoirs

A thirty-year simulation period of 1981 to 2010 was chosen. The Cauvery and Narmada Basins were disaggregated into 444 and 653 modelling cells, respectively. Both basins included domestic, irrigation, and livestock demand (with the inclusion of industrial demand limited to the Cauvery due to data limitations in the Narmada), large-scale water transfers, hydropower reservoirs, irrigation reservoirs, and agriculture within the command and rural areas.

2.5. Model Calibration

Several gauges were included within each basin for the purpose of calibration: 14 in the Cauvery and 13 in the Narmada (Figure 1). Simulated streamflow was calibrated against observed streamflow using the SIMPLEX auto-calibration routine. This routine utilises four parameters (a surface and groundwater routing parameter, a Probability Distributed Model (PDM) parameter that describes the spatial variation in soil moisture capacity, and a multiplier to adjust rooting depths). The calibration gauges were selected based on the completeness of the data, time of the data, and size of the sub-catchment. The observed data were deemed sufficient when more than 50% of the values were identified as "observed" and not "computed" and had at least five consecutive years available from 1981 until 2010. Additionally, sub-catchments smaller than 800 km^2 (six GWAVA grid cells) were nested into the larger sub-catchment in which they are located.

The reservoir outflow parameters were manually calibrated. Table 1 presents the parameters for each reservoir that provided the best fit to either observed outflow-data, where available, or downstream observed streamflow.

Table 1. Reservoir outflow parameters determined by a manual calibration for each major reservoir in the Cauvery and Narmada basins.

Reservoir	Basin	Capacity (10^9 m^3)	Simulated Average Annual Inflow (10^{10} m^3/Year)	c	Equation	α	β
Hemavathy	Cauvery	0.99	0.22	0.45	5	0.7	0.8
Krishna Raja Sagara (KRS)	Cauvery	1.016	0.35	0.29	5	0.7	1
Kabini	Cauvery	0.44	0.15	0.29	5	0.1	1
Bhavanisagar	Cauvery	0.791	0.09	0.86	4	1	
Mettur	Cauvery	2.64	0.70	0.38	5	1	0.1
Bargi	Narmada	3.18	0.32	1.01	4	0.3	
Barna	Narmada	0.539	0.21	0.26	5	0.3	0.3
Tawa	Narmada	2.313	0.27	0.86	4	0.3	
Indira Sagar Project (ISP)	Narmada	10	3.03	0.33	5	0.1	1
Omkareshwar Sagar Project (OSP)	Narmada	0.987	1.40	0.07	5	0.1	1
Sardar Sarovar Project (SSP)	Narmada	9.5	3.69	0.26	5	0.5	0.3
Karjan	Narmada	0.63	3.89	0.02	5	0.1	0.3

3. Model Evaluation

Due to the high variability of streamflow in both the Cauvery and Narmada basins, several different metrics are used to quantify the model performance under various flow regimes. In this study, the Kling- Gupta Efficiency (*KGE*) was used to determine the models' ability to represent the entirety of the hydrograph, the Nash-Sutcliffe Efficiency (*NSE*) to determine the model performance in representing the high flow periods, the Log-Nash Efficiency (*LNE*) was used to determine the model's performance in representing the low-flow periods, and the bias was used to evaluate the model ability to estimate the total volume of streamflow across the modelling period. The change in model skill was utilised

to compare the performance of two model configurations (GWAVA and GWAVA-GW, GWAVA and GWAVA-Res, and GWAVA and GWAVA 5.1).

3.1. Kling-Gupta Efficiency (KGE)

The *KGE* is based on correlation, variability bias, and mean bias, and is calculated as follows:

$$KGE = 1 - \sqrt{(r-1)^2 + \left(\frac{\sigma_s}{\sigma_o} - 1\right)^2 + \left(\frac{\mu_s}{\mu_o} - 1\right)^2} \tag{6}$$

where r is the correlation coefficient between the simulated and observed data, σ_o is the standard deviation of observation data, σ_s is the standard deviation of the simulated data, μ_o is the mean of observation data, and μ_s is the mean of simulated data.

The *KGE* indicates the overall performance of the model. The metric allows some perceived shortcomings with *NSE* to be overcome and has become increasingly popular for the evaluation of hydrological model skill. A *KGE* of one indicates perfect agreement between simulations and observations. However, there are many opinions as to where the differentiation of "good" and "-poor" model performance thresholds lie within the *KGE* scale. Negative *KGE* values do not always imply that the model performs worse than the mean flow benchmark. For this study, and to be able to compare model performance, a *KGE* score of less than 0.2 was deemed poor, between 0.2 and 0.6 was fair, and above 0.6 was good.

3.2. Nash-Sutcliffe Efficiency (NSE)

NSE is a popular metric to evaluate hydrological model performance because it normalises model performance into an interpretable scale, and was calculated as follows:

$$NSE = 1 - \frac{\sum_{t=1}^{T}\left(Q_s^t - Q_o^t\right)^2}{\sum_{t=1}^{T}\left(Q_o^t - \overline{Q_o}\right)^2} \tag{7}$$

where Q_s^t and Q_o^t are, respectively, the simulated streamflow, and the observed streamflow at time-step t; $\overline{Q_o}$ is the average observed streamflow over all timesteps considered.

An *NSE* of one represents a perfect correspondence between the simulations and observations. An *NSE* of zero indicates that the model simulations have the same explanatory power as the mean of the observations. An *NSE* of less than zero represents that the model is a worse predictor than the mean of the observations. However, *NSE* does not provide an equal benchmark for different flow regimes. Utilising the single *NSE* metric is not sufficient for determining the performance of a model, however, it can provide context if utilised in conjunction with additional model performance efficiencies. For this study, an *NSE* score of less than 0.2 was deemed poor, between 0.2 and 0.6 was fair, and above 0.6 was good.

3.3. Log-Nash Efficiency (LNE)

LNE is used for model evaluation when low-flow performance is of importance and was calculated as follows:

$$LNE = 1 - \frac{\sum_{t=1}^{T}\left(Q_{s\_log}^t - Q_{o\_log}^t\right)^2}{\sum_{t=1}^{T}\left(Q_{o\_log}^t - \overline{Q_{o\_log}}\right)^2} \tag{8}$$

With the following:

$$Q_{s\_log}^t = log_{10}\left(Q_s^t + c\right) \tag{9}$$

$$Q_{o\_log}^t = log_{10}\left(Q_o^t + c\right) \tag{10}$$

where $Q_{s\_log}^t$ and $Q_{o\_log}^t$ are, respectively, the log of simulated streamflow, and the log of observed streamflow at time-step t; $\overline{Q_{o\_log}}$ is the average of log-observed streamflow over

all timesteps considered. c is a positive constant equal to the 10th percentile of the observed flow. The use of the constant c reduced emphasis on negligible flows, which tend to be unreliable, and avoids numerical problems with attempting to calculate the logarithm of zero flows. The *LNE* was interpreted in the same way as the *NSE*.

3.4. Bias

The bias is the average tendency of the simulated data to over-or under-estimate the observed data (Equation (11)). The optimal value for the bias is zero. Positive values indicate a model under-estimation and negative values indicate an over-estimation. When assessing a model's ability to simulate streamflow, the bias indicates the ability of the model to predict the overall streamflow volume across the modelling period.

$$Bias = \frac{\sum_{t=1}^{T}(y_o - y_s)}{\sum_{t=1}^{n} y_o} \times 100 \tag{11}$$

where y_o is the observed data value, y_s is the simulated data value, and t is the time-step.

3.5. Model Skill

The change in model skill, $\Delta skill$, between the different model configurations for streamflow prediction was calculated as follows:

$$\Delta skill = \frac{R_2 - R_1}{R_{optimal} - R_1} \tag{12}$$

where R_1 and R_2 are the efficiency values for the two model configurations being compared and $R_{optimal}$ is the best possible efficiency value for a given metric. A positive value of $\Delta skill$ indicates that model configuration two performs better than model configuration one, a zero value suggests similar performance, and a negative value demonstrates that model configuration two performs less well than model configuration one.
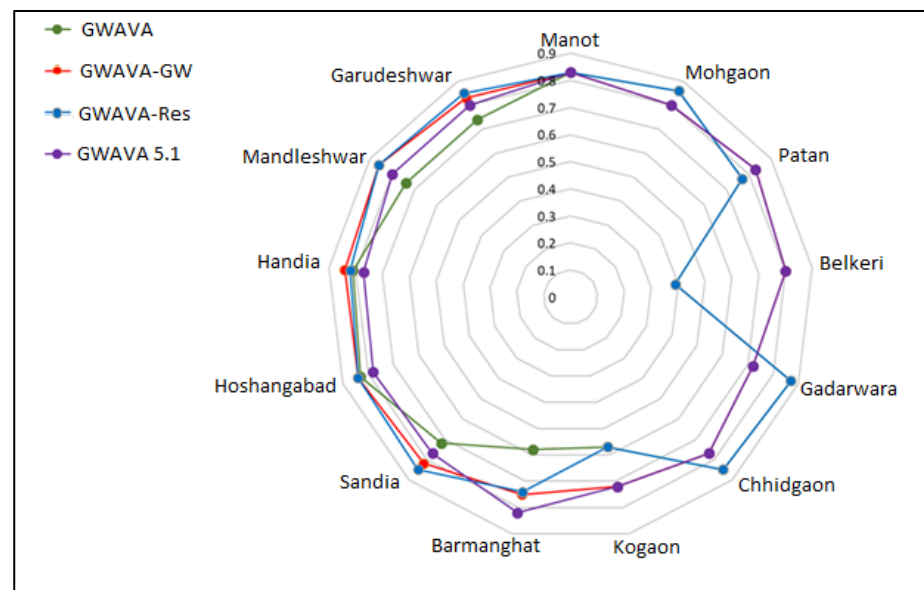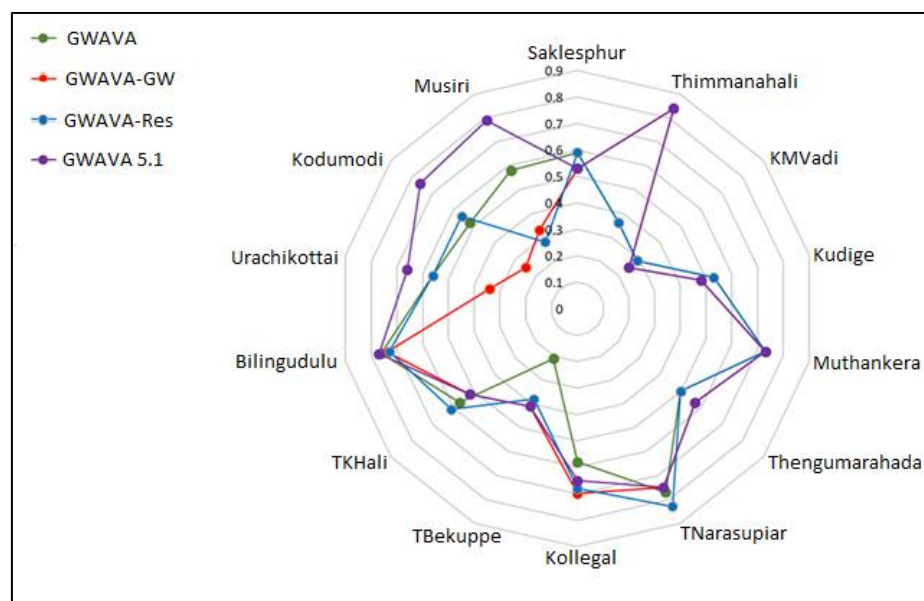
4. Results

4.1. Streamflow

The ability of the four model versions to predict the observed streamflow was presented through the monthly *KGE* at each gauging station (Figure 3), to demonstrate the model's overall performance, and as an indication of the model's skill in representing the low-flows (Figures 3 and 4). The monthly bias, *NSE*, *KGE*, and *LNE* values for each sub-catchment for each model version can be found in Table A3 in Appendix B

The model performance was higher in the Narmada compared to the Cauvery. In the sub-catchments of the Cauvery and Narmada, GWAVA 5.1 outperforms GWAVA. However, the performance of GWAVA-GW and GWAVA-Res varies between the sub-catchments. As expected, in sub-catchments without major reservoirs, GWAVA produced the same results as GWAVA-Res, and GWAVA-GW produced the same results as GWAVA 5.1.

All the simulated flows for the sub-catchments in the Narmada are classified as "good" in performance, except for the simulation of Belkeri without the groundwater routine, which was classified as "fair" (Figure 3). In the Cauvery, the results are more varied, with eight sub-catchments classified as good and six sub-catchments as fair when using GWAVA 5.1. The performance of the downstream sub-catchments, without the combination of groundwater and the regulated reservoir routine, falls within the fair range (Figure 4).
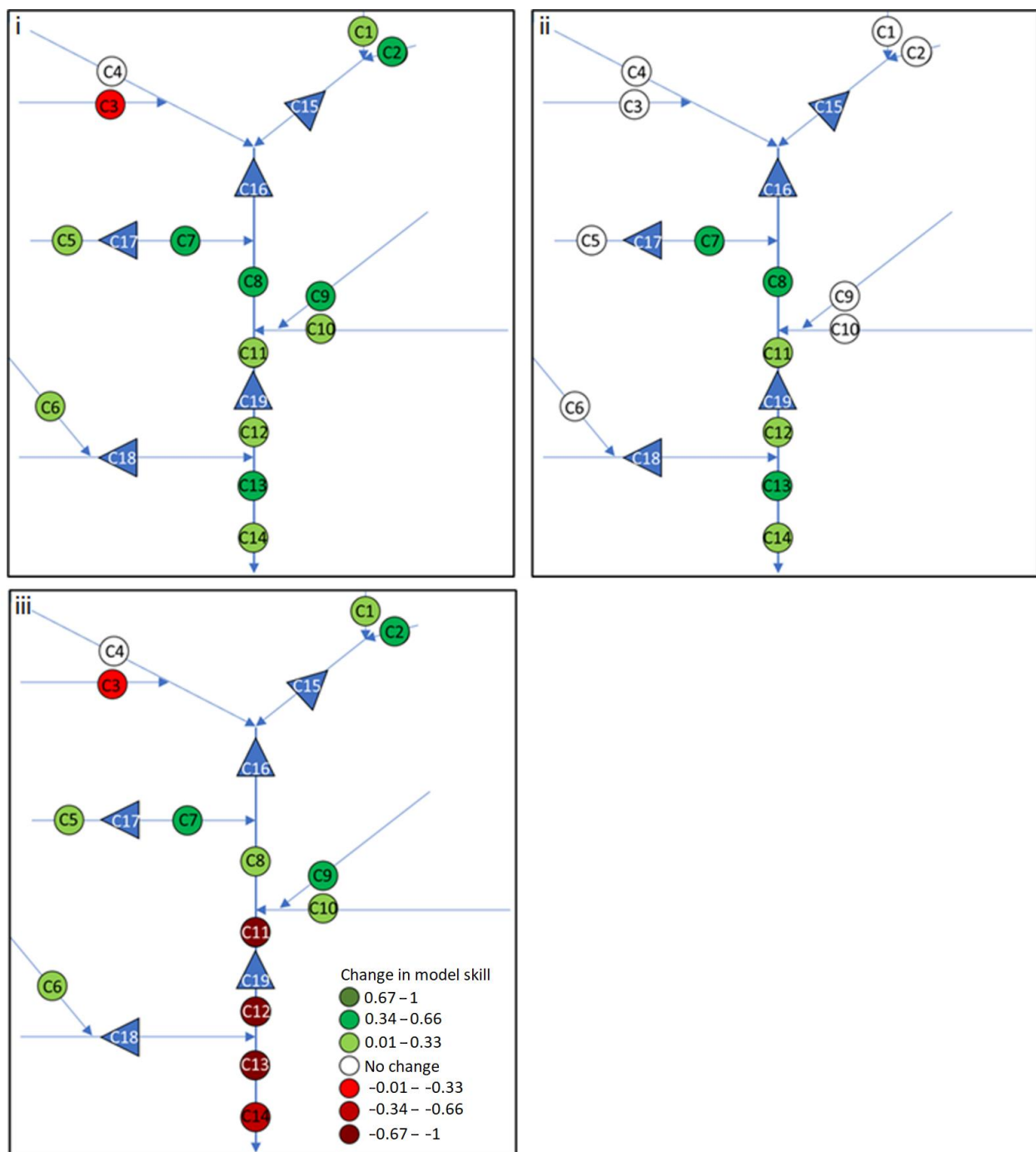
Figure 3. A representation of the monthly *KGE* values obtained for each model at each gauging station within the Narmada Basin. The values on the y-axis represent the *KGE* value.

Figure 4. A representation of the monthly *KGE* values obtained for each model at each gauging station within the Cauvery Basin. The values on the y-axis represent the *KGE* value.
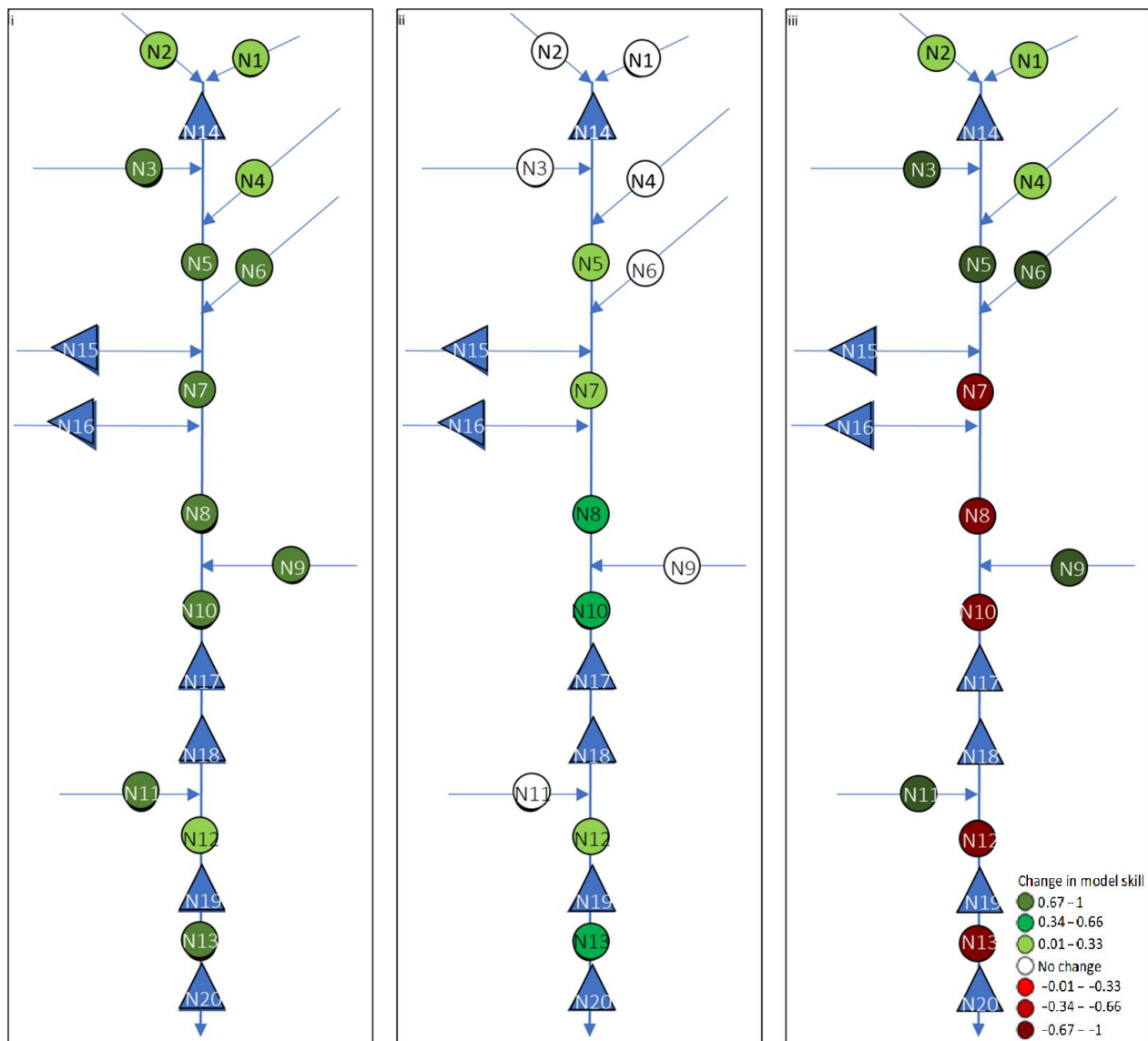
The ability of the model to represent the low-flow periods well is critical in basins that suffer from water scarcity. In the Cauvery Basin, the aggressive pumping of groundwater limits the baseflow released from the groundwater store to sustain the streamflow in the dry season, and the large reservoirs store and release water in contrast to the seasonal patterns. The inclusion of groundwater feedback into GWAVA improves the simulation of the low-flows within the headwater sub-catchments, which is critical when assessing water resources and surface water-groundwater interactions (Figure 5iii). The incorporation of the regulated reservoir module allows for the release of water in the dry season. The reservoir module markedly improves the simulation downstream of these major reservoirs in the Cauvery (Figure 5ii). The combination of the groundwater processes and inclusion of the regulated reservoirs improves the ability of GWAVA to represent the low-flows throughout the basin (Figure 5i).

Figure 5. A representation of the low-flow model skill for each sub-catchment in the Cauvery Basin for the (**i**) GWAVA 5.1, (**ii**) GWAVA-Res, and (**iii**) GWAVA- GW versions, compared to GWAVA.

The Narmada River is primarily groundwater-fed following the monsoon. Understanding the baseflow contribution to streamflow and the impact that the large reservoirs have on the dry season flow poses a challenge for water managers. The inclusion of the groundwater module improves the model's representation of the low-flows within the headwater sub-catchments (Figure 6iii). The inclusion of the groundwater processes allows the model to better retain water within the groundwater store and release baseflow throughout the year. The large reservoirs within the Narmada consistently release water through the hydropower plants, and thus the incorporation of the regulated reservoir routine allows the model to release water from the reservoirs throughout the year. The

regulated reservoir routine produces a better match to the observed low-flow-data periods compared to results using the original GWAVA reservoir routine (Figure 6ii). The dual incorporation of the groundwater processes and the regulated reservoir routine provides a better representation of the low-flow periods across the basin (Figure 6i).
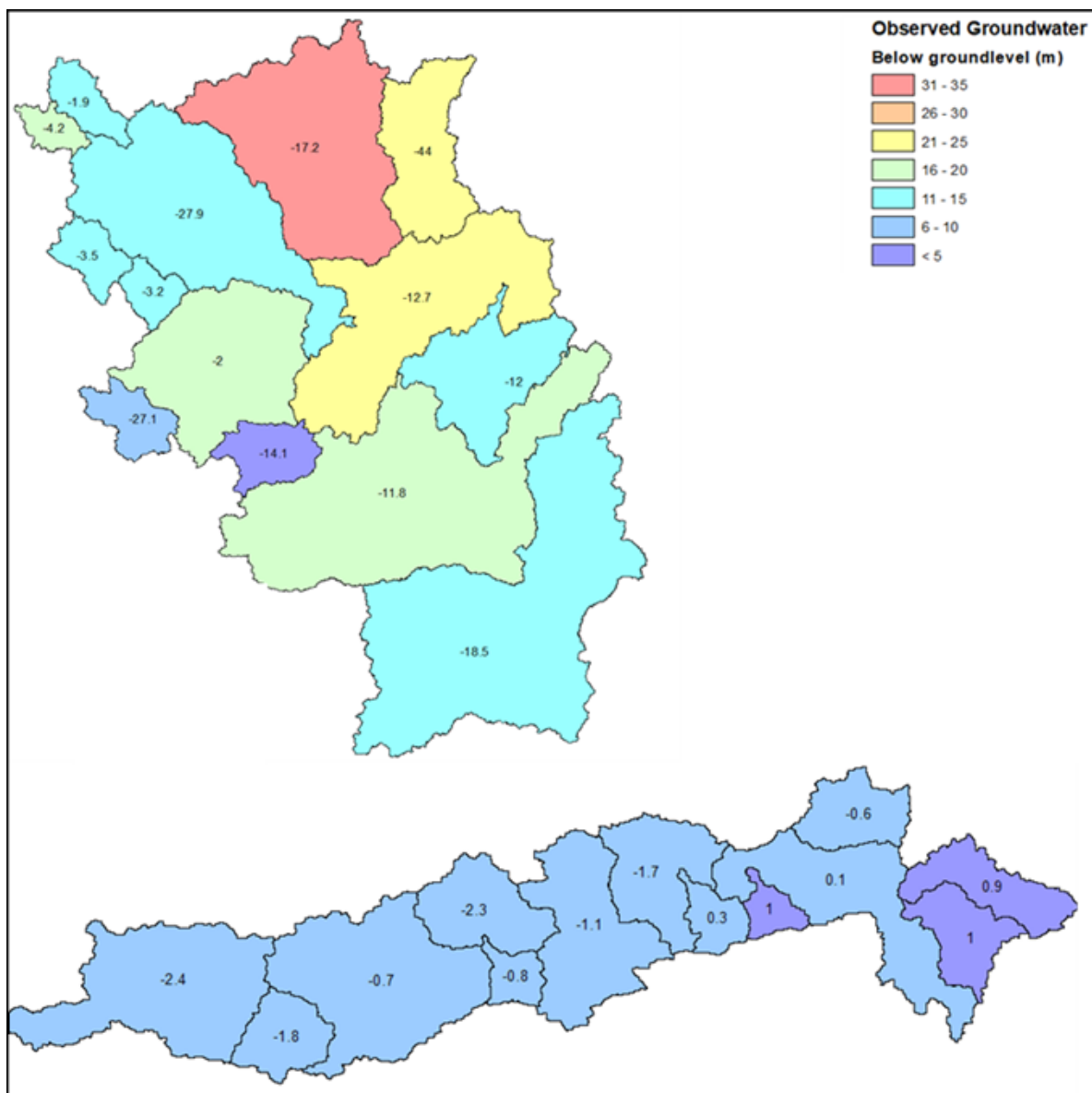

Figure 6. A representation of the low-flow model's skill for each sub-catchment in the Narmada Basin for the (**i**) GWAVA 5.1, (**ii**) GWAVA-Res, and (**iii**) GWAVA-GW versions, compared to GWAVA.

4.2. Groundwater

The average observed depth to groundwater (measured from ground level) is deeper in the Cauvery than in the Narmada (Figure 7). In the Cauvery, the wetter, more pristine sub-catchments along the western boundary (Western Ghats) have a shallower observed groundwater-level (5 to 10 m below ground level), while the groundwater-level deepens (11 to 35 m below ground level) throughout the remainder of the basin. In the Cauvery, GWAVA 5.1 can represent shallower groundwater-levels with higher accuracy compared to deeper levels, however, it systematically over-estimates the depth to groundwater throughout the basin.

Figure 7. Average observed groundwater-levels below ground level (legend), and the difference between the observed and GWAVA 5.1 simulated groundwater-levels in meters (numerical values on maps), from 1981 to 2010 for the Narmada and Cauvery sub-catchments.

The average observed groundwater depth within the Narmada basin is no deeper than 10 m below the ground level. GWAVA 5.1 can represent the average groundwater-levels well throughout the sub-catchments, with the observed average differing a maximum of two meters from the simulated average in the most downstream sub-catchment. The representation was more accurate in the upstream sub-catchments where the water table is shallower, and the landscape is less degraded.

4.3. Reservoirs

In the Narmada, GWAVA represents the daily reservoir releases well but over-estimates the total volume of water released at Bargi, Tawa, and SSP (Table 2). The inclusion of the regulated reservoir routine in the Narmada did not significantly improve the daily release representation but did improve the total volume of water being released over the simulation period. In the Cauvery, GWAVA represents daily release well at Kabini and KRS, but poorly at Mettur. The total volume of water released from the major reservoirs in the
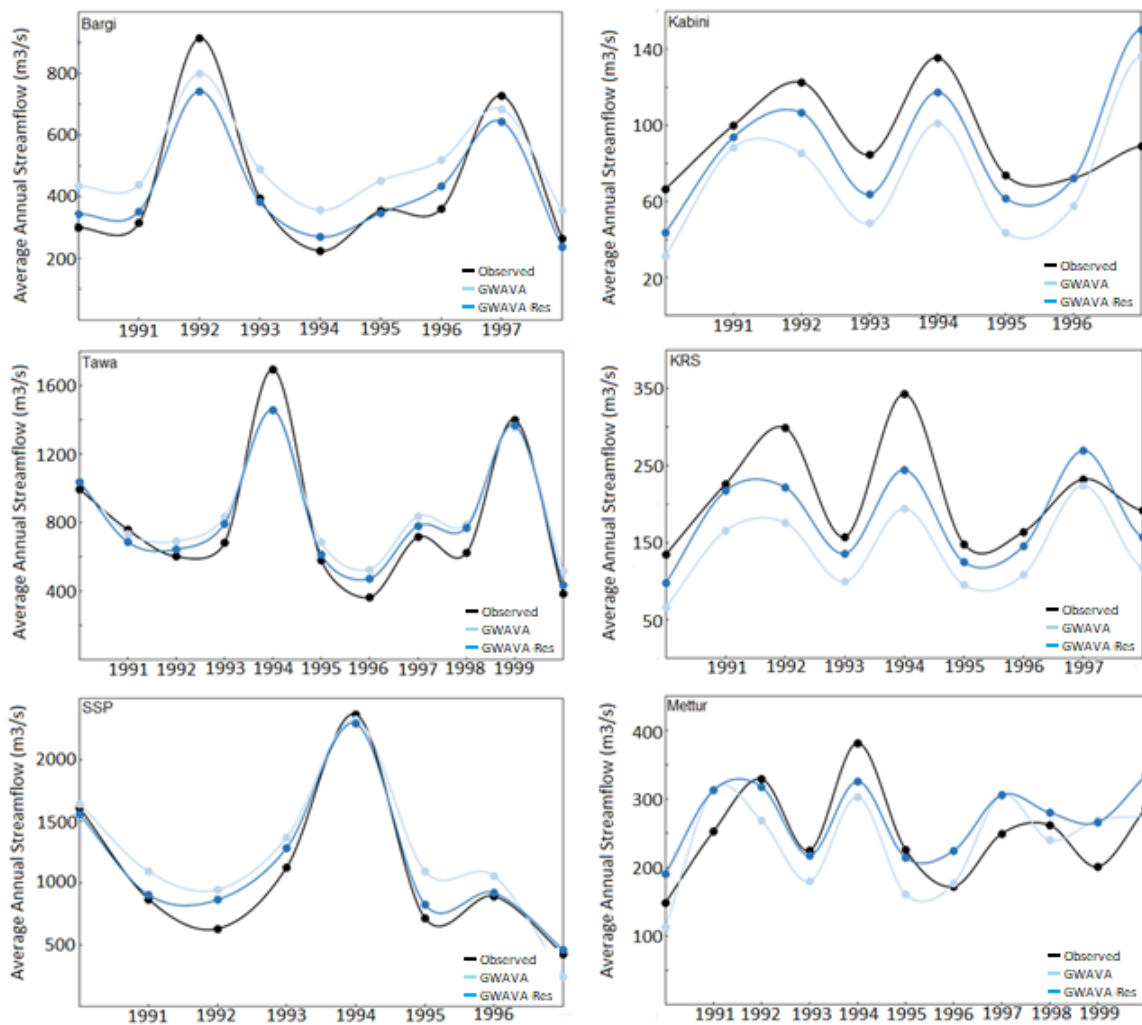
Cauvery is under-estimated. When applying the regulated reservoir routine, the daily releases and total volume of water released are significantly improved (Table 2).

Table 2. The percent bias and daily Nash- Sutcliffe Efficiency (*NSE*) at the outlets of the major reservoirs for GWAVA and GWAVA-Res.
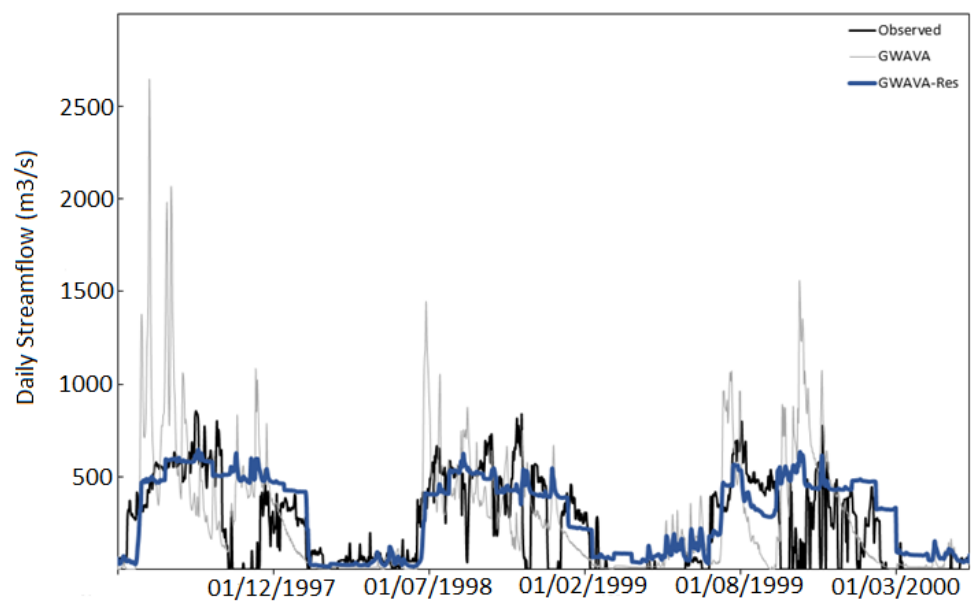
Reservoir Outlet	Bias (%)		Daily *NSE*	
	GWAVA	**GWAVA-Res**	**GWAVA**	**GWAVA-Res**
Bargi	17.8	3.2	0.53	0.62
Tawa	7.57	0.4	0.74	0.7
SSP	16.09	4.35	0.62	0.65
Kabini	−13.45	3.64	0.37	0.59
KRS	−33.69	−15.43	0.38	0.52
Mettur	−4.69	9.35	−0.25	0.39

The application of the regulated reservoir routine better represents the annual reservoir releases throughout the observational time period at Kabini, Tawa, KRS, and SSP (Figure 8). At Bargi, GWAVA-Res simulates the normal and dry years better than GWAVA, but under-estimates the annual releases in wet years (Figure 8). The annual releases are improved until 1995 at Mettur dam, but following 1995, GWAVA-Res has a better temporal pattern and GWAVA a better representative release volume (Figure 8). Although the annual volume at Mettur was better represented by GWAVA, at the daily scale, GWAVA-Res can capture the regulated reservoir pattern significantly better than GWAVA (Figure 9).
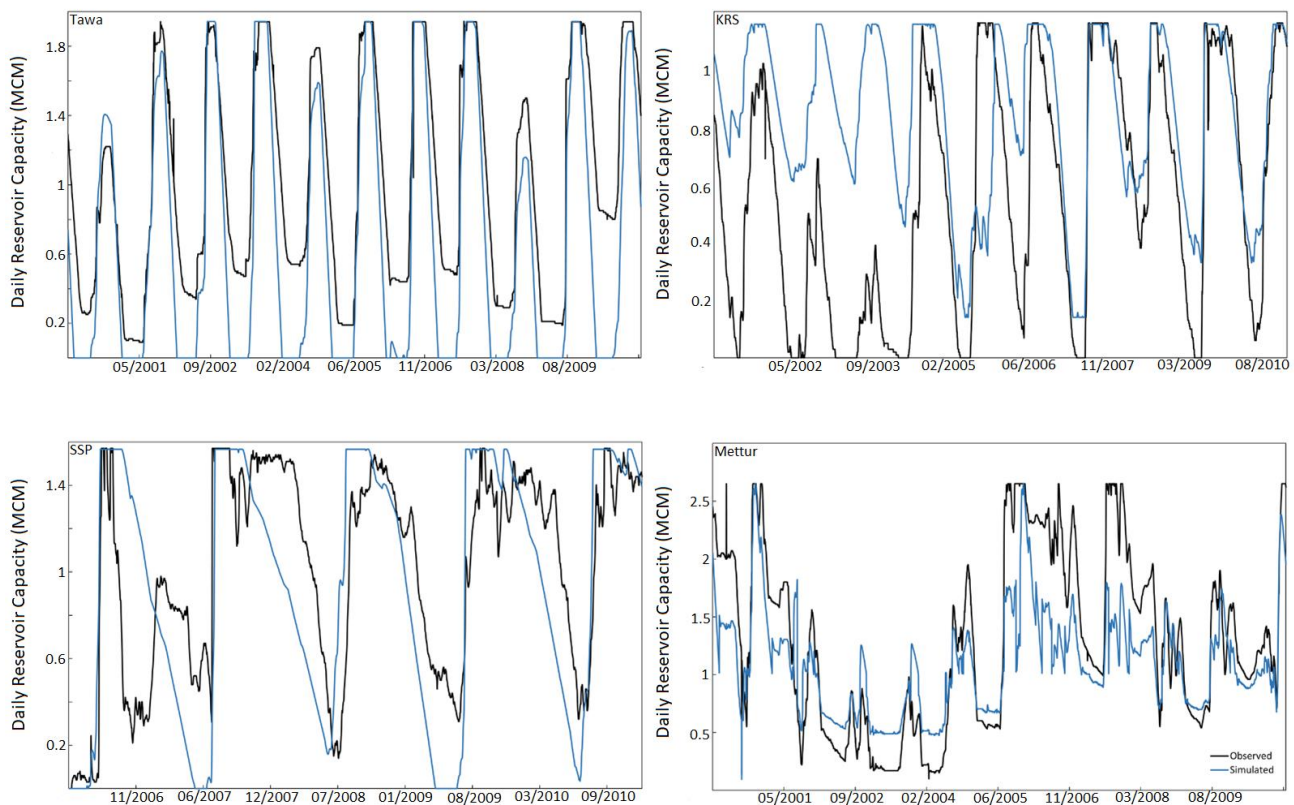
GWAVA 5.1 represents the daily reservoir capacity during the monsoon period well at Tawa and SSP. The model was depleting the reservoir storage through irrigation demand during the dry seasons, which was not reflected in the observed data. The filling and release temporal patterns were good at Tawa, accurately reflecting the observational data (Figure 10). At SSP, the model tends to reach full capacity and begin releasing water earlier in the monsoon than suggested by the observed data (Figure 10). At KRS, the observed data demonstrate a depletion or near-depletion of reservoir storage during the dry season. The model, however, was overestimating the volume of water remaining in the reservoir during these times. GWAVA 5.1 does not capture the 2002–2003 drought period particularly well in the upper regions of the basin (Figure 10). At the Mettur Dam, the model produces a satisfactory temporal pattern; however, it over-estimates the volume in the dry season and under-estimates it in the monsoon. The 2002–2003 drought was better captured by the model in this reservoir compared to the upper regions of the basin (Figure 10).

Figure 8. Average annual observed and GWAVA and GWAVA-Res simulated reservoir releases at the outflow of Bargi, Tawa, SSP, Kabini, KRS, and Mettur reservoirs.

Figure 9. Daily observed and GWAVA and GWAVA-Res simulated reservoir outflows at the outflow of Mettur Dam.

Figure 10. Observed and GWAVA 5.1 simulated daily reservoir storage in million cubic meters for Tawa, KRS, and Mettur, and billion cubic meters for SSP, across varying periods for which observed data were available.

5. Discussion

The revision of the groundwater routine allows for the traceability of recharge, base-flow, groundwater-levels, and volume of abstraction from groundwater resources. The regulated reservoir routine allows for a release from the major reservoirs throughout the year and the output of reservoir storage capacity throughout the simulation period. The improved groundwater and reservoir routines were included in the GWAVA model, with the addition of three and two input parameters, respectively.

The inclusion of the revised groundwater routine improved the simulation of stream-flow in the headwater catchments, while the new reservoir routine improved the simulation of streamflow in catchments downstream of major reservoirs in both the Cauvery and Narmada. The regulated reservoir routine improves both the timing and volume of re-leases from major reservoirs. In line with GWAVA 5.1, revisions to the reservoir routines in SWAT [62], DHSVM [17], VIC [63], MESH [25], and HYPE [26] improved representation and parameterization of major operational reservoir outflows, illustrating that such revisions in large-scale models can benefit both temporal and volumetric simulation of streamflow downstream of reservoirs. GWAVA 5.1 can track the reservoir capacity through-out the simulation period. In the Narmada, seasonality and filling of Tawa and SSP are well represented; however, the model was drying out the reservoirs each year, which was not reflected in reality. It is therefore necessary to introduce a user-defined limit into the reservoir routine to restrict extraction and release below a realistic reservoir level. In the Cauvery, at KRS, the opposite were occurring. The observed reservoir levels are reducing to empty each year, but the model was simulating water in the reservoirs during this time. At the Mettur Dam, the daily reservoir capacity was highly sensitive to the volume of inflow. Although the temporal pattern was adequate, the model was overestimating the volume of water in the reservoir during the dry season but underestimating the volume during the monsoon.

The streamflow in the Narmada is primarily base flow fed [64], and groundwater pumping is limited to periods of drought. The groundwater tends to fluctuate within ten meters of the ground level. The model accurately represented the average groundwater depth within two meters of the observed average over the simulation period. The inclusion of more comprehensive groundwater processes within the model structures allows for a more accurate simulation of the hydrograph within the Narmada, especially during the dry season.

Thomas et al. (2021) [64] applied SWAT in the Upper Narmada. This study allowed irrigation demands to be met from shallow and deep aquifer stores. The reservoir simulation required the engineering particulars of the reservoir and inflows into the reservoir to estimate the probable flow at 50%, 75%, and 90% dependability for different months. In the headwater catchments, GWAVA and GWAVA 5.1 outperform SWAT in the prediction of streamflow. The original and revised groundwater routines with the original reservoir equation perform well within these catchments where the reservoirs are small and the steep topography results in the overland flow being the dominant streamflow generation process. At Barmanghat, downstream of Bargi Dam (regulated reservoir) and with a larger base flow contribution, SWAT performs better than GWAVA, but with the inclusion of the more comprehensive groundwater and regulated reservoirs, GWAVA 5.1 performs better than SWAT.

Goswami and Kar (2018) [65] represented the full extent of the Narmada basin using a version of SWAT, where groundwater flow contribution to streamflow was simulated by routing through a shallow aquifer store, but with no considerations for reservoirs within the basin. GWAVA-GW and GWAVA 5.1 significantly outperform SWAT in streamflow prediction at Garudeshwar. Pechlivanidis and Arheimer (2015) [66] applied India-HYPE in the Narmada basin using a 15-parameter reservoir routine and a comprehensive, multi-parameter, groundwater routine. All the versions of GWAVA presented in this study outperform India-HYPE at Garudeshwar. The average groundwater depth estimations by GWAVA 5.1 in the Hoshangabad district of Madhya Pradesh are consistent with those simulated using a conceptual groundwater model by Nema et al. (2019) [67].

The satisfactory performance of GWAVA 5.1 to represent streamflow, groundwater-levels, and reservoir fluxes throughout the basin, compared with observed data and existing literature, demonstrates the value of the simple, low input routines incorporated into GWAVA. Therefore, the inclusion of groundwater processes and regulation reservoirs was justified when modelling basins with natural and anthropogenic characteristics similar to that of the Narmada.

In the upper regions of the Cauvery, ANN [32,68], SWAT [34], and VIC [34] outperform both GWAVA and GWAVA 5.1, although the performance of GWAVA was improved when the groundwater routine was applied to this region. GWAVA 5.1 underestimated the aquifer level across the basin. Collins et al. (2020) [69] demonstrated largely under-simulated groundwater-levels compared to the observed data in the Berambadi sub-catchment of the Cauvery, using a one-dimensional numerical transect model. It was suggested that a poor representation of the India Meteorological Department (IMD) rainfall in this region is a critical part of the poor simulations of both recharge to groundwater and streamflow in this region [33].

Quantifying and managing uncertainty is a significant challenge in large-scale modelling. The model structure allocates water to evaporative components first, and thus, the evaporative processes are favoured in times of water stress. Along with the use of the Hargreaves evaporation estimation method, the model architecture is one of the fundamental reasons for the under-estimation of streamflow during the dry season.

The one-dimensional groundwater representation may not represent the groundwater processes in regions with highly depleted aquifers and gneiss geomorphology as well as those with underlying shale. The non-uniformity of the groundwater observation network in both Narmada and Cauvery is a source of uncertainty for accurate calibration of the

model. The conversion of point well data to a spatial average could be a significant source of uncertainty, as groundwater-levels tend to be highly dynamic across small areas.

The simplified approach to representing the outflows of the regulated reservoirs has proven largely valid, but inevitably carries uncertainty as actual reservoir operations are more complex and highly individual. Although a more complex module could have been incorporated, data availability and the fundamental low-data principle of GWAVA were carefully considered. The performance of the modified Hanasaki routine is largely dependent on the quality of the observed reservoir outflow or downstream streamflow used in the calibration. In regions of poor data quality, the performance of the routine could be compromised. Although the reservoir routine utilises daily inflows and consistently updates reservoir storage, determining two parameters that influence reservoir outflow over a period of time could cause stationarity issues when modelling future time periods.

Uncertainty arises from observation station mechanical errors and spatial distribution, and various spatial and temporal interpolation methods. At some gauging points in the basin, there is low confidence in the observed streamflow and reservoir outflow-data. On occasion, the reservoir outflow-data do not resemble streamflow records in close proximity downstream. Eye-witness accounts and some literature report drying out of streams in the dry season, which is not reflected in the observed data. Additionally, in reality, rivers downstream of significant urban and agricultural areas are often fed by a perennial stream of human or livestock sewage [33]. Although the model represents return flows from domestic demand, this may be under-estimated compared to the volume of effluent being released into these rivers in reality.

The IMD gridded precipitation and temperature data are provided in a 0.5-degree grid. Each 0.5-degree grid cell contains numerous terrain and gradient increments, and the grid cells may fall over the basin boundary. This results in an inaccurate representation of the distribution and total rainfall, and the distribution of the minimum and maximum temperature in this region of the basin [33,34]. There is a known source of uncertainty within the Western Ghats region, which acts as the headwaters for the larger Cauvery Basin.

GWAVA 5.1 potentially over-estimates water withdrawals in basins, particularly in the Cauvery, where the exact anthropogenic water use was uncertain and poorly documented. The depth to groundwater depends on the estimated water withdrawal of the region. The potential over-estimation of demand could cause the early or complete depletion of wells, not reflected in reality. The cost and availability of electricity are not considered within GWAVA and thus does not form a realistic constraint when modelling the process of groundwater abstraction. The under-estimation of the groundwater-levels and subsequent base flow component hinders the ability of the model to accurately represent the streamflow. There were low confidence in the data concerning the pumping depth and observed groundwater-level data in this region [30,70].

When improving a low-data input hydrological model, such as GWAVA, caution must be taken to not complicate the model beyond its underlying capability. The improvements to GWAVA utilising simple modified routines demonstrate that adapting existing hydrological models can be suitable for the improvement in the reliability of streamflow, reservoir, and groundwater prediction.

6. Conclusions

Robust simulations of groundwater availability and reservoir storage and releases are important for water resource management in semi-arid basins, where the groundwater was an important water source during the dry season and streamflow in the main channel of the lower reaches was largely reservoir-regulated.

The main conclusions from this study are:

- Key components of GWAVA were improved to better represent water management, while maintaining low input data requirements and model complexity.
- The model improvements successfully improved model performance in both the Narmada and Cauvery basins.

- Simulated groundwater and reservoir storage levels were output to gain further insight into components of the basin water balance.

Although these simplified routines improve model performance throughout the basin, it is recommended that further application in a wider geographic area is necessary, to ensure the new routines suitability represent a range of basin characteristics. Investigation into multiple parameter configurations would assist in quantifying uncertainty, and potentially improve abstractions and release parameters.

Appendix A

Table A1. The spatial and temporal resolutions, periods, and sources of the input data used in the set-up of GWAVA in the Cauvery (C) and Narmada (N) basins.

Input Data	Basin	Spatial Resolution	Temporal Resolution	Time Period	Source
Precipitation	C, N	0.25 degree	Daily	1951–2017	Indian Meteorological Department [71]
Maximum temperature	C, N	0.25 degree	Daily	1951–2016	Indian Meteorological Department [71]
Minimum temperature	C, N	0.25 degree	Daily	1951–2016	Indian Meteorological Department [71]
Streamflow gauged data	C, N	Basin	Daily	1971–2014	Water Resources Information System of India (India-WRIS) https://indiawris.gov.in/wris/#/ (accessed on 22 December 2018)
Reservoir characteristics	C N	Basin Basin		2018 2020	India-WRIS Narmada Control Authority, India-WRIS

Table A1. *Cont.*

Input Data	Basin	Spatial Resolution	Temporal Resolution	Time Period	Source
Reservoir inflow and outflow-data	C N	Basin Basin	Monthly Monthly	1974–2017 2007–2017	India-WRIS Narmada Control Authority
Reservoir storage	C, N	Basin	Daily	200–2010	India-WRIS
Water transfers	C	Basin	Annual	2008	Ashoka Trust for Research in Ecology and the Environment
	N	Basin	Annual	2009	Narmada Control Authority
Groundwater levels	C, N	District	Monthly	1990–2017	Central Groundwater Board, India
Elevation	C, N	0.003 degree		2000	NASA Shuttle Radar Mission Global 1 arc second V003 [72]
Geology	C, N	Asia			United States Geological Survey
Specific yield	C, N	India			Central Groundwater Board, India
Soil type	C	0.008 degree		1971–1981	Harmonized World Soil Database v1.2 [73]
	N	1:10,000		1958–2020	Soil and Land-use Survey of India https://www.india.gov.in/website-soil-and-land-use-survey-india (accessed on 7 April 2019)
Soil properties	C, N	Global		2010	Table 2—Allen et al. (2010) [74]
Land Cover Land Use	C, N	0.001 degree		2005	Decadal land-use and land cover across India 2005 [75]
Crops	C N	Taluk 5 arcmin		2000 2010	National Remote Sensing Centre (NRSC) Portmann (2010) [76]
Total and Rural Population	C, N	Village		2001	Census of India 2001 (http://sedac.ciesin.columbia.edu/data/set/india-india-village-level-geospatial-socio-econ-1991--2001) (accessed on 17 March 2019)
Livestock	C	0.05 degree		2005	CGIR Livestock of the World v2 [77]
	N	Rural villages, India		2012	19th Livestock Census-2012. Government of India
Conveyance losses	C, N	Village		2011	Household & Irrigation Census 2011-Town and Village directory (https://censusindia.gov.in/DigitalLibrary/TablesSeries2001.aspx) (accessed on 17 March 2019)
Return flow	C, N	Village		2011	Household & Irrigation Census 2011-Town and Village directory (https://censusindia.gov.in/DigitalLibrary/TablesSeries2001.aspx) (accessed on 17 March 2019)
Irrigation efficiency	C, N	Continental		1986	Irrigation and Drainage Paper (FAO) No 1
Surface- water fraction	C	Village		2011	Household & Irrigation Census 2011-Town and Village directory (https://censusindia.gov.in/DigitalLibrary/TablesSeries2001.aspx) (accessed on 17 March 2019)
	N	5 arcmin		2013	Global Map of Irrigation Areas-version 5.0 http://www.fao.org/aquastat/en/geospatial-information/global-maps-irrigated-areas/map-quality (accessed on 7 April 2019)
Industrial demand	C	Karnataka		Currently unknown	Industrial Plot Information System-Karnataka Industrial Area Development Board (https://http://164.100.133.168/kiadbgisportal/) (accessed on 17 March 2019)

Input Data	Basin	Spatial Resolution	Temporal Resolution	Time Period	Source
Livestock demand	C, N	India		2006	FAO (2018) [78]
Domestic demand	C	Village		2001	Household & Irrigation Census 2011-Town and Village directory (https://censusindia.gov.in/DigitalLibrary/TablesSeries2001.aspx) (accessed on 17 March 2019)
	N	India			AQUASTAT [78]

Table A2 presents the demand constraints selected for each basin. These values were derived from the Indian Decadal Census and the Indian Irrigation Census.

Table A2. Input Demand Constraints for the Cauvery and Narmada Basins.

Demand Constraints	Cauvery	Narmada
Conveyance loss (%)—Urban	23	15
Conveyance loss (%)—Rural	25	15
Irrigation Efficiency (%)	44	70
Return flow (%)—Urban	62	45
Return flow (%)—Rural	0	45
Demand per head (L/d)—Cattle	77	40
Demand per head (L/d)—Sheep and goat	5	4
Surface water abstraction (%)—Urban	44	57
Surface water abstraction (%)—Rural	62	57
Surface water abstraction (%)—Industrial	80	80
Surface water abstraction (%)—Irrigation	31	47

Appendix B

Table A3. The percent bias, monthly Nash-Sutcliffe Efficiency (*NSE*), monthly log-Nash Efficiency (*LNE*), and the monthly Kling-Gupta Efficiency (*KGE*) for each sub-catchment in the Narmada and Cauvery basins. The metrics are provided for GWAVA (G), GWAVA-GW (G-GW), GWAVA-Res (G-Res), and GWAVA 5.1 (G 5.1).

Sub-Catchment	Bias (%)				Monthly *NSE*				Monthly *LNE*				Monthly *KGE*			
	G	G-GW	G-Res	G 5.1	G	G-GW	G-Res	G 5.1	G	G-GW	G-Res	G 5.1	G	G-GW	G-Res	G 5.1
								Narmada								
Manot	11.37	4.24	11.37	4.24	0.95	0.92	0.92	0.93	0.78	0.86	0.78	0.86	0.83	0.84	0.83	0.83
Mohgaon	2.77	8.26	2.77	3.4	0.87	0.83	0.83	0.83	0.73	0.85	0.73	0.85	0.86	0.8	0.86	0.8
Patan	17.17	−0.77	17.17	12.3	0.9	0.83	0.83	0.91	0.59	0.83	0.59	0.91	0.77	0.75	0.77	0.83
Belkeri	33.9	2.94	33.9	2.46	0.84	0.85	0.85	0.84	0.6	0.62	0.6	0.71	0.39	0.81	0.39	0.8
Gadarwara	7.03	−1.8	7.03	1	0.92	0.82	0.82	0.83	−0.45	0.71	−0.45	0.83	0.87	0.7	0.87	0.72
Chhidgaon	−12.36	−45	−12.36	−13.29	0.89	0.62	0.62	0.86	−0.33	0.66	−0.33	0.88	0.85	0.6	0.85	0.77
Kogaon	30.39	−19.5	30.39	2.03	0.79	0.74	0.74	0.79	−0.32	0.68	−0.32	0.76	0.57	0.66	0.57	0.72
Barmanghat	17.8	3.9	−2.88	3.2	0.74	0.7	0.82	0.81	0.51	0.78	0.8	0.81	0.58	0.75	0.74	0.82
Sandia	6.73	7.55	3.24	9.11	0.84	0.77	0.93	0.84	0.51	−0.04	0.84	0.88	0.72	0.82	0.85	0.77
Hoshangabad	7.57	−0.68	2.92	0.4	0.89	0.82	0.94	0.9	0.08	−0.94	0.85	0.90	0.83	0.84	0.84	0.78
Handia	14	4.75	11.17	9.92	0.89	0.82	0.95	0.91	−0.33	−1.94	0.84	0.90	0.81	0.84	0.82	0.77
Mandleshwar	10.6	4.25	4.73	4.35	0.9	0.84	0.95	0.92	0.71	−1.25	0.85	0.88	0.74	0.86	0.86	0.80
Garudeshwar	16.09	12.74	4.43	13.4	0.9	0.78	0.94	0.9	0.18	−1.8	0.84	0.89	0.74	0.83	0.85	0.80
								Cauvery								
Saklesphur	−37	−46.4	−37	−46.4	0.77	0.57	0.77	0.57	0.31	0.81	0.31	0.81	0.59	0.53	0.59	0.53
Thimmanahali	−58.1	−3.6	−58.1	−3.6	0.21	0.71	0.21	0.71	0.34	0.58	0.34	0.58	0.36	0.84	0.36	0.84
KMVadi	−21	−50.3	−21	−50.3	0.21	0.14	0.21	0.14	0.14	−0.07	0.14	−0.07	0.29	0.25	0.29	0.25

Table A3. *Cont.*

Sub-Catchment	Bias (%)				Monthly *NSE*				Monthly *LNE*				Monthly *KGE*			
	G	G-GW	G-Res	G 5.1	G	G-GW	G-Res	G 5.1	G	G-GW	G-Res	G 5.1	G	G-GW	G-Res	G 5.1
Kudige	−43	−50.7	−43	−50.7	0.67	0.55	0.67	0.55	0.70	0.70	0.70	0.70	0.53	0.48	0.53	0.48
Munthankera	−21.6	−25.4	−21.6	−25.4	0.8	0.78	0.8	0.78	0.74	0.89	0.74	0.89	0.73	0.73	0.73	0.73
Thengumarahada	1.2	−22.3	1.2	−22.3	0.07	0.43	0.07	0.43	0.22	0.59	0.22	0.59	0.50	0.57	0.50	0.57
T narasupiar	−13.4	−12.0	3.6	−11.6	0.66	0.6	0.75	0.6	−9.83	−1.6	−0.4	−1.2	0.77	0.75	0.83	0.75
Kollegal	−33.6	−16.9	−15.4	−24.9	0.54	0.56	0.70	0.56	−7.46	−2.18	0.69	0.56	0.58	0.7	0.68	0.65
Tbekuppe	2.6	−5.4	−12	−5.4	−0.81	−0.09	0.62	0.49	−23.97	−0.72	0.53	−0.72	0.21	0.41	0.38	0.41
TKHali	4.1	7.3	3.4	7.3	0.36	0.43	0.4	0.43	−1.68	−0.29	−0.91	−0.29	0.57	0.52	0.61	0.52
Bilingudulu	−14.7	−2.2	12.1	−10.5	0.63	0.5	0.79	0.64	0.07	−0.77	0.69	0.65	0.76	0.74	0.73	0.77
Urachikottai	−4.6	−11.5	21.0	9.3	0.09	−0.35	0.13	0.57	0.07	−0.77	0.69	0.71	0.56	0.34	0.56	0.66
Kodumodi	−14.5	−22.7	20.0	−5.9	0.14	−0.3	0.52	0.64	−1.56	−3.80	0.41	0.51	0.52	0.25	0.56	0.76
Musiri	−5.8	−6.8	18.2	−2.1	0.15	−0.45	0.14	0.66	−0.81	−1.69	−0.12	0.37	0.58	0.33	0.28	0.79

References

1. Döll, P.; Douville, H.; Güntner, A.; Schmied, H.M.; Wada, Y. Modelling Freshwater Resources at the Global Scale, Challenges and Prospects. *Surv. Geophys.* **2016**, *37*, 195–221. [CrossRef]
2. Vorosmarty, C.J.; Hoekstra, A.Y.; Bunn, S.E.; Conway, D.; Gupta, J. Fresh Water Goes Global. *Science* **2015**, *349*, 478–479. [CrossRef] [PubMed]
3. Liu, Y.; Gupta, H.; Springer, E.; Wagener, T. Linking Science with Environmental Decision Making, Experiences from An Integrated Modelling Approach to Supporting Sustainable Water Resources Management. *Environ. Model. Softw.* **2008**, *23*, 846–858. [CrossRef]
4. Kingston, D.; Massei, N.; Dieppois, B.; Hannah, D.; Hartmann, A.; Lavers, D.; Vidal, J.P. Moving Beyond the Catchment Scale, Value and Opportunities in Large-Scale Hydrology to Understand Our Changing World. *Hydrol. Process.* **2020**, *34*, 2292–2298. [CrossRef]
5. Famiglietti, J.S. The Global Groundwater Crisis. *Nat. Clim. Chang.* **2014**, *4*, 945–948. [CrossRef]
6. Mackellar, N.C.; Dadson, S.J.; New, M.; Wolski, P. Evaluation of the JULES Land-Surface Model in Simulating Catchment Hydrology in Southern Africa. *Hydrol. Earth Syst. Sci. Discuss.* **2013**, *10*, 11093–11128.
7. Clark, M.P.; Fan, Y.; Lawrence, D.M.; Adam, J.C.; Bolster, D.; Gochis, D.J.; Hooper, R.P.; Kumar, M.; Leung, L.R.; Mackay, D.S.; et al. Improving the Representation of Hydrologic Processes in Earth System Models. *Water Resour. Res.* **2015**, *51*, 5929–5956. [CrossRef]
8. Pokhrel, Y.N.; Hanasaki, N.; Wada, Y.; Kim, H. Recent Progresses in incorporating Human Land–Water Management into Global Land-Surface Models toward their integration into Earth System Models. *Wiley Interdiscip. Rev. Water* **2016**, *3*, 548–574. [CrossRef]
9. Scheidegger, J.M.; Jackson, C.R.; Muddu, S.; Tomar, S.K.; Filgueira, R. integration of 2D Lateral Groundwater Flow into the Variable infiltration Capacity (VIC) Model and Effects on Simulated Fluxes for Different Grid Resolutions and Aquifer Diffusivities. *Water* **2021**, *13*, 663. [CrossRef]
10. Hanasaki, N.; Yoshikawa, S.; Pokhrel, Y.; Kanae, S. A Global Hydrological Simulation to Specify the Sources of Water Used by Humans. *Hydrol. Earth Syst. Sci.* **2018**, *22*, 789–817. [CrossRef]
11. Sutanudjaja, E.H.; Van Beek, R.; Wanders, N.; Wada, Y.; Bosmans, J.H.; Drost, N.; Van Der Ent, R.J.; De Graaf, I.E.; Hoch, J.M.; De Jong, K.; et al. PCR-GLOBWB 2, A 5 Arcmin Global Hydrological and Water Resources Model. *Geosci. Model Dev.* **2018**, *11*, 2429–2453. [CrossRef]
12. Burek, P.; Satoh, Y.; Kahil, T.; Tang, T.; Greve, P.; Smilovic, M.; Guillaumot, L.; Zhao, F.; Wada, Y. Development of the Community Water Model (Cwatm V1. 04)–A High-Resolution Hydrological Model for Global and Regional Assessment of integrated Water Resources Management. *Geosci. Model Dev.* **2020**, *13*, 3267–3298. [CrossRef]
13. Müller Schmied, H.; Cáceres, D.; Eisner, S.; Flörke, M.; Herbert, C.; Niemann, C.; Peiris, T.A.; Popat, E.; Portmann, F.T.; Reinecke, R.; et al. The Global Water Resources and Use Model Watergap V2. 2d, Model Description and Evaluation. *Geosci. Model Dev.* **2021**, *14*, 1037–1079. [CrossRef]
14. Droppers, B.; Franssen, W.H.; Van Vliet, M.T.; Nijssen, B.; Ludwig, F. Simulating Human Impacts on Global Water Resources Using VIC-5. *Geosci. Model Dev.* **2020**, *13*, 5029–5052. [CrossRef]
15. Harbaugh, A.W. *MOD-FLOW-2005, the US Geological Survey Modular Groundwater Model, the Groundwater Flow Process*; US Geological Survey: Reston, VA, USA, 2005.
16. Downing, J.A.; Prairie, Y.T.; Cole, J.J.; Duarte, C.M.; Tranvik, L.J.; Striegl, R.G.; Mcdowell, W.H.; Kortelainen, P.; Caraco, N.F.; Melack, J.M.; et al. The Global Abundance and Size Distribution of Lakes, Ponds, and Impoundments. *Limnol. Oceanogr.* **2006**, *51*, 2388–2397. [CrossRef]
17. Zhao, G.; Gao, H.; Naz, B.S.; Kao, S.C.; Voisin, N. integrating A Reservoir Regulation Scheme into A Spatially Distributed Hydrological Model. *Adv. Water Resour.* **2016**, *98*, 16–31. [CrossRef]

18. Haddeland, I.; Skaugen, T.; Lettenmaier, D.P. Anthropogenic Impacts on Continental Surface Water Fluxes. *Geophys. Res. Lett.* **2006**, *33*, 1–4. [CrossRef]

19. Döll, P.; Kaspar, F.; Lehner, B. A Global Hydrological Model for Deriving Water Availability indicators, Model Tuning and Validation. *J. Hydrol.* **2003**, *270*, 105–134. [CrossRef]

20. Hanasaki, N.; Kanae, S.; Oki, T. A Reservoir Operation Scheme for Global River Routing Models. *J. Hydrol.* **2006**, *327*, 22–41. [CrossRef]

21. Hanasaki, N.; Kanae, S.; Oki, T.; Masuda, K.; Motoya, K.; Shirakawa, N.; Shen, Y.; Tanaka, K. An integrated Model for the Assessment of Global Water Resources–Part 1, Model Description and input Meteorological forcing. *Hydrol. Earth Syst. Sci.* **2008**, *12*, 1007–1025. [CrossRef]

22. Biemans, H.; Haddeland, I.; Kabat, P.; Ludwig, F.; Hutjes, R.W.; Heinke, J.; Von Bloh, W.; Gerten, D. Impact of Reservoirs on River Discharge and Irrigation Water Supply During the 20th Century. *Water Resour. Res.* **2011**, *47*, 1–15. [CrossRef]

23. Chen, J.; Wu, Y. Advancing Representation of Hydrologic Processes in the Soil and Water Assessment Tool (SWAT) through the integration of the topographic MODEL (TOPMODEL) Features. *J. Hydrol.* **2012**, *420*, 319–328. [CrossRef]

24. Yassin, F.; Razavi, S.; Elshamy, M.; Davison, B.; Sapriza-Azuri, G.; Wheater, H. Representation and Improved Parameterization of Reservoir Operation in Hydrological and Land-Surface Models. *Hydrol. Earth Syst. Sci.* **2019**, *23*, 3735–3764. [CrossRef]

25. Tefs, A.A.; Stadnyk, T.A.; Koenig, K.A.; Dery, S.J.; Macdonald, M.K.; Slota, P.; Crawford, J.; Hamilton, M. Simulating River Regulation and Reservoir Performance in A Continental-Scale Hydrologic Model. *Environ. Model. Softw.* **2021**, *141*, 105025. [CrossRef]

26. Meigh, J.R.; Mckenzie, A.A.; Sene, K.J. A Grid-Based Approach to Water Scarcity Estimates for Eastern and Southern Africa. *Water Resour. Manag.* **1999**, *13*, 85–115. [CrossRef]

27. Madhusoodhanan, C.G.; Sreeja, K.G.; Eldho, T.I. Climate Change Impact Assessments on the Water Resources of India under Extensive Human interventions. *Ambio* **2016**, *45*, 725–741. [CrossRef] [PubMed]

28. Sharma, A.; Hipel, K.W.; Schweizer, V. Strategic insights into the Cauvery River Dispute in India. *Sustainability* **2020**, *12*, 1286. [CrossRef]

29. Hoekstra, A.Y.; Mekonnen, M.M.; Chapagain, A.K.; Mathews, R.E.; Richter, B.D. Global Monthly Water Scarcity, Blue Water Footprints versus Blue Water Availability. *PLoS ONE* **2012**, *7*, e32688.

30. Bhave, A.G.; Conway, D.; Dessai, S.; Stainforth, D.A. Water Resource Planning Under Future Climate and Socioeconomic Uncertainty in the Cauvery River Basin in Karnataka, India. *Water Resour. Res.* **2018**, *54*, 708–728. [CrossRef] [PubMed]

31. Falkenmark, M.; Molden, D. Wake Up to Realities of River Basin Closure. *Int. J. Water Resour. Dev.* **2008**, *24*, 201–215. [CrossRef]

32. Patel, S.S.; Ramachandran, P. A Comparison of Machine Learning Techniques for Modelling River Flow Time Series, The Case of Upper Cauvery River Basin. *Water Resour. Manag.* **2015**, *29*, 589–602. [CrossRef]

33. Horan, R.; Wable, P.S.; Srinivasan, V.; Baron, H.E.; Keller, V.J.; Garg, K.K.; Rickards, N.; Simpson, M.; Houghton-Carr, H.A.; Rees, H.G. Modelling Small-Scale Storage interventions in Semi-Arid India at the Basin Scale. *Sustainability* **2021**, *13*, 6129. [CrossRef]

34. Horan, R.; Gowri, R.; Wable, P.S.; Baron, H.; Keller, V.D.; Garg, K.K.; Mujumdar, P.P.; Houghton-Carr, H.; Rees, G. A Comparative Assessment of Hydrological Models in the Upper Cauvery Catchment. *Water* **2021**, *13*, 151. [CrossRef]

35. Raju, B.K.; Nandagiri, L. Assessment of Variable Source Area Hydrological Models in Humid Tropical Watersheds. *Int. J. River Basin Manag.* **2018**, *16*, 145–156. [CrossRef]

36. Gosain, A.K.; Rao, S.; Basuray, D. Climate Change Impact Assessment on Hydrology of Indian River Basins. *Curr. Sci.* **2006**, *90*, 346–353.

37. Singh, A.; Gosain, A.K. Climate Change Impact Assessment Using GIS-Based Hydrological Modelling. *Water Int.* **2011**, *36*, 386–397. [CrossRef]

38. Bhuvaneswari, K.; Geethalakshmi, V.; Lakshmanan, A.; Srinivasan, R.; Sekhar, N.U. the Impact of El Nino/Southern Oscillation on Hydrology and Rice Productivity in the Cauvery Basin, India, Application of the Soil and Water Assessment Tool. *Weather Clim. Extrem.* **2013**, *2*, 39–47. [CrossRef]

39. Mandal, U.; Sahoo, S.; Munusamy, S.B.; Dhar, A.; Panda, S.N.; Kar, A.; Mishra, P.K. Delineation of Groundwater Potential Zones of Coastal Groundwater Basin Using Multi-Criteria Decision Making Technique. *Water Resour. Manag.* **2016**, *30*, 4293–4310. [CrossRef]

40. Geetha, K.; Mishra, S.K.; Eldho, T.I.; Rastogi, A.K.; Pandey, R.P. SCS-CN-Based Continuous Simulation Model for Hydrologic forecasting. *Water Resour. Manag.* **2008**, *22*, 165–190. [CrossRef]

41. Parvez, M.B.; Inayathulla, M. Estimation of Surface Runoff by Soil Conservation Service Curve Number Model for Upper Cauvery Karnataka. *Int. J. Sci. Res. Multidiscip. Stud.* **2019**, *5*, 11.

42. Raje, D.; Priya, P.; Krishnan, R. Macroscale Hydrological Modelling Approach for Study of Large-Scale Hydrologic Impacts Under Climate Change in Indian River Basins. *Hydrol. Process.* **2014**, *28*, 1874–1889. [CrossRef]

43. Gupta, H.; Chakrapani, G.J. Temporal and Spatial Variations in Water Flow and Sediment Load in Narmada River Basin, India, Natural and Man-Made Factors. *Environ. Geol.* **2005**, *48*, 579–589. [CrossRef]

44. Thomas, T.; Gunthe, S.S.; Ghosh, N.C.; Sudheer, K.P. Analysis of Monsoon Rainfall Variability Over Narmada Basin in Central India, Implication of Climate Change. *J. Water Clim. Chang.* **2015**, *6*, 615–627. [CrossRef]

45. Nayak, T.; Verma, M.K.; Bindu, S.H. SCS Curve Number Method in Narmada Basin. *Int. J. Geomat. Geosci.* **2012**, *3*, 219–228.

46. Rai, P.K.; Chaubey, P.K.; Mohan, K.; Singh, P. Geoinformatics for Assessing the inferences of Quantitative Drainage Morphometry of the Narmada Basin in India. *Appl. Geomat.* **2017**, *9*, 167–189. [CrossRef]

47. Jain, S.K.; Storm, B.; Bathurst, J.C.; Refsgaard, J.C.; Singh, R.D. Application of the SHE to Catchments in India Part 2. Field Experiments and Simulation Studies with the SHE on the Kolar Subcatchment of the Narmada River. *J. Hydrol.* **1992**, *140*, 25–47. [CrossRef]

48. Gajbhiye, S.; Mishra, S.K.; Pandey, A. Effects of Seasonal/Monthly Variation on Runoff Curve Number for Selected Watersheds of Narmada Basin. *Int. J. Environ. Sci.* **2013**, *3*, 2019–2030.

49. Khare, D.; Patra, D.; Mondal, A.; Kundu, S. Impact of Land-use/Land Cover Change on Runoff in the Catchment of a Hydro Power Project. *Appl. Water Sci.* **2017**, *7*, 787–800. [CrossRef]

50. Pathan, H.; Joshi, G.S. Estimation of Runoff Using SCS-CN Method and Arcgis for Karjan Reservoir Basin. *Int. J. Appl. Eng. Res.* **2019**, *14*, 2945–2951.

51. Tiwari, D.; Tiwari, H.L.; Saini, R. Hydrological Modelling in Narmada Basin Using Remote Sensing and GIS with SWAT Model and Runoff Prediction in Patan Watershed. *Int. J. Adv. Res. Ideas Innov. Technol.* **2018**, *4*, 344–352.

52. Rickards, N.; Thomas, T.; Kaelin, A.; Houghton-Carr, H.; Jain, S.K.; Mishra, P.K.; Nema, M.K.; Dixon, H.; Rahman, M.M.; Horan, R.; et al. Understanding Future Water Challenges in A Highly Regulated Indian River Basin—Modelling the Impact of Climate Change on the Hydrology of the Upper Narmada. *Water* **2020**, *12*, 1762. [CrossRef]

53. Tomer, S.K.; Al Bitar, A.; Sekhar, M.; Zribi, M. MAPSM: A Spatio-Temporal Algorithm for Merging Soil Moisture from Active and Passive Microwave Remote Sensing. *Remote Sens.* **2016**, *8*, 990. [CrossRef]

54. Mcdonald, M.G.; Harbaugh, A.W. *A Modular Three-Dimensional Finite-Difference Groundwater Flow Model*; US Geological Survey: Reston, VA, USA, 1988.

55. Subash, Y.; Sekhar, M.; Tomer, S.; Sharma, A. A Framework for Assessment of Climate Change Impacts on the Groundwater System. In *Sustainable Water Resources Management*; American Society of Civil Engineers: Reston, VA, USA, 2016.

56. Mondal, A.; Narasimhan, B.; Sekhar, M.; Mujumdar, P.P. Hydrologic Modelling. *Proc. Indian Natl. Sci. Acad. Part A Phys. Sci.* **2016**, *82*, 817–832. [CrossRef]

57. Sekhar, M.; Riotte, J.; Ruiz, L.; Jouquet, P.; Braun, J.J. Influences of Climate and Agriculture on Water and Biogeochemical Cycles, Kabini Critical Zone Observatory. *Proc. Indian Natl. Sci. Acad.* **2016**, *82*, 833–846. [CrossRef]

58. Robert, M.; Thomas, A.; Sekhar, M.; Raynal, H.; Casellas, É.; Casel, P.; Chabrier, P.; Joannon, A.; Bergez, J.É. A Dynamic Model for Water Management at the Farm Level integrating Strategic, Tactical and Operational Decisions. *Environ. Model. Softw.* **2018**, *100*, 123–135. [CrossRef]

59. De Bruin, A.; De Condappa, D.; Mikhail, M.; Tomer, S.K.; Sekhar, M.; Barron, J. Simulated Water Resource Impacts and Livelihood Implications of Stakeholder-Developed Scenarios in the Jaldhaka Basin, India. *Water Int.* **2012**, *37*, 492–508. [CrossRef]

60. Baron, H.; Keller, V.; Horan, R.; Houghton-Carr, H.; Rees, G.; Collins, S.; Jackson, C.; Mujumdar, P.; Muddu, S.; Rajendran, R. Estimating current and future groundwater resources across the Cauvery basin using a macro-scale gridded water-resource model. In *EGU General Assembly Conference Abstracts*; European Geosciences Union: Munich, Germany, 2020.

61. Hanasaki, N.; Inuzuka, T.; Kanae, S.; Oki, T. An Estimation of Global Virtual Water Flow and Sources of Water withdrawal for Major Crops and Livestock Products Using a Global Hydrological Model. *J. Hydrol.* **2010**, *384*, 232–244. [CrossRef]

62. Wu, Y.; Chen, J. An Operation-Based Scheme for a Multiyear and Multipurpose Reservoir to Enhance Macroscale Hydrologic Models. *J. Hydrometeorol.* **2012**, *13*, 270–283. [CrossRef]

63. Wang, K.; Shi, H.; Chen, J.; Li, T. An Improved Operation-Based Reservoir Scheme integrated with Variable infiltration Capacity Model for Multiyear and Multipurpose Reservoirs. *J. Hydrol.* **2019**, *57*, 365–375. [CrossRef]

64. Thomas, T.; Ghosh, N.C.; Sudheer, K.P. Optimal Reservoir Operation–A Climate Change Adaptation Strategy for Narmada Basin in Central India. *J. Hydrol.* **2021**, *598*, 126238. [CrossRef]

65. Goswami, S.B.; Kar, S.C. Simulation of Water Cycle Components in the Narmada River Basin by forcing SWAT Model with CFSR Data. *Meteorol. Hydrol. Water Manag. Res. Oper. Appl.* **2018**, *6*, 13–25. [CrossRef]

66. Pechlivanidis, I.G.; Arheimer, B. Large-Scale Hydrological Modelling by Using Modified PUB Recommendations, the India-HYPE Case. *Hydrol. Earth Syst. Sci.* **2015**, *19*, 4559–4579. [CrossRef]

67. Nema, S.; Awasthi, M.K.; Nema, R.K. Conceptual Groundwater Modelling in an Alluvial Aquifer of Upper Narmada Basin. *J. Soil Water Conserv.* **2019**, *18*, 179–187. [CrossRef]

68. Maheswaran, R.; Khosa, R. Wavelet–Volterra Coupled Model for Monthly Stream Flow forecasting. *J. Hydrol.* **2012**, *450*, 320–335. [CrossRef]

69. Collins, S.L.; Loveless, S.E.; Muddu, S.; Buvaneshwari, S.; Palamakumbura, R.N.; Krabbendam, M.; Lapworth, D.J.; Jackson, C.R.; Gooddy, D.C.; Nara, S.N.; et al. Groundwater Connectivity of a Sheared Gneiss Aquifer in the Cauvery River Basin, India. *Hydrogeol. J.* **2020**, *28*, 1371–1388. [CrossRef]

70. Hora, T.; Srinivasan, V.; Basu, N.B. the Groundwater Recovery Paradox in South India. *Geophys. Res. Lett.* **2019**, *46*, 9602–9611. [CrossRef]

71. Pai, D.S.; Rajeevan, M.; Sreejith, O.P.; Mukhopadhyay, B.; Satbha, N.S. Development of a New High Spatial Resolution (0.25 × 0.25) Long Period (1901–2010) Daily Gridded Rainfall Data Set Over India and Its Comparison with Existing Data Sets Over the Region. *Mausam* **2014**, *65*, 1–8.

72. NASA Jet Propulsion Laboratory (JPL), NASA Shuttle Radar Topography Mission Global 1 Arc Second Number, National Aeronautics and Space Administration, U.S. Government, NASA. Pasadena, CA, USA. 2013. Available online: https://www2.jpl.nasa.gov/srtm/ (accessed on 20 October 2018).

73. Fischer, G.; Nachtergaele, F.; Prieler, S.; Van Velthuizen, H.; Verelst, L.; Wiberg, D. *Global Agro-Ecological Zones Assessment for Agriculture*; International Institute for Applied Systems Analysis, Food and Agriculture Organization of the United Nations: Laxenburg, Austria; Rome, Italy, 2008; pp. 26–31.

74. Allen, D.M.; Cannon, A.J.; Toews, M.W.; Scibek, J. Variability in Simulated Recharge Using Different GCMS. *Water Resour. Res.* **2010**, *46*, 1–18.

75. Roy, P.S.; Meiyappan, P.; Joshi, P.K.; Kale, M.P.; Srivastav, V.K.; Srivasatava, S.K.; Behera, M.D.; Roy, A.; Sharma, Y.; Ramachandran, R.M.; et al. *Decadal Land Use and Land Cover Classifications Across India, 1985, 1995, 2005*; ORNL DAAC: Oak Ridge, TN, USA, 2016.

76. Portmann, F.T.; Siebert, S.; Döll, P. MIRCA2000—Global Monthly Irrigated and Rainfed Crop Areas Around the Year 2000, A New High-Resolution Data Set for Agricultural and Hydrological Modelling. *Glob. Biogeochem. Cycles* **2010**, *24*, 1–24. [CrossRef]

77. Robinson, T.P.; Wint, G.W.; Conchedda, G.; Van Boeckel, T.P.; Ercoli, V.; Palamara, E.; Cinardi, G.; D'Aietti, L.; Hay, S.I.; Gilbert, M. Mapping the Global Distribution of Livestock. *PLoS ONE* **2014**, *9*, e96084. [CrossRef]

78. Food and Agriculture Organization of the United Nations, AQUASTAT. Food and Agriculture Organization of the United Nations. Available online: http://www.Fao.Org/Aquastat/Statistics/Query/index.Html?Lang=En (accessed on 19 January 2019).